Title
In Vitro Studies of Steriodogenic Factor-1 Sumoylation, a Post-translational Modification Critical for Adrenal and Gonadal Development

Author
Lontok, Erik Tugna

Publication Date
2011

Peer reviewed|Thesis/dissertation

In Vitro Studies of Steriodogenic Factor-1 Sumoylation, a Post-translational Modification Critical for Adrenal and Gonadal Development

by

Erik Tugna Lontok

DISSERTATION

Submitted in partial satisfaction of the requirements for the degree of

DOCTOR OF PHILOSOPHY

in

Biochemistry

in the

GRADUATE DIVISION

of the

Acknowledgements

Graduate school has been one of the most arduous endeavors I have ever undertaken in my life. I could list the failed experiments or maybe the pointless ideas that all deserved to die in their own quiet way, yet I feel that would still do a disservice in describing just how hard this experience truly was. I take comfort in that this Sisyphean task was made bearable and possible by the wonderful people I have met along the way. From my supportive dissertation committee and especially my graduate advisor, Dr. Holly Ingraham, for seeing in this student someone worth salvaging, educating and ushering into this world as a confident, self-assured professional. Words cannot express how thankful I am for the opportunity and guidance that Holly has provided. It is a testament to how fine of a mentor Holly is, in that she figured out how to motivate me. The Ingraham lab members constitute some of the finest, most professional and wonderful people I have ever had the pleasure of knowing. Their sense of camaraderie and desire to perform the best possible science, daily reminds me of what the ideal laboratory situation is. I would like to especially note Dr. Raymond Blind, my immediate mentor and teacher when I first joined the lab. Ray's ability to clearly explain complex biochemical theories and processes are what led me to undertake and succeed in earning my Biochemistry degree.

Beyond UCSF, I draw inspiration from my family and though I hardly visited them, I don't think they understand how rejuvenating and empowering the times I spend with them are. In their daily actions and struggles, I see before my eyes what true responsibility and maturity looks like. It is sobering to think that beyond these walls, far

removed from experiments, lab meetings, posters and high-minded discussions lies Life. And that this life is rarely fair and hardly easy. Yet there they go, everyday, without a second thought about what time it is, or how much they have to do that day. “I don’t have time to worry, I have too much to do,” would say my mother. I cannot think of a finer example of a role model than my mother. To truly understand devotion, determination, and love one need only spend a day with her. She has been an inspiration, an aspiration and truly the greatest friend I have ever had. For all that I am and all that I will ever achieve, I will always have her to thank.

And lastly, I would like to acknowledge Dr. Katherine Sorber, my partner, my fiancée and someday soon my wife. Of all the wonderful things that have happened to me and of all the interesting people I have met, no one, nothing comes close to being as great as what Katherine has been for me. I know I can make people laugh, but it is Katherine that makes me laugh. And cry. And angry. And thoughtful. And every shade of the emotional spectrum. If I had to do this all over again, knowing what I know now, I would not hesitate for a heartbeat if only to know that at the end of it, I would come out with Katherine Sorber.

Abstract

Steroidogenic Factor-1 (SF-1) is a constitutively active nuclear hormone receptor, thus its post-translational modifications play an even more important role in its regulation. SF-1 is sumoylated at two sites, K119 and K194 of which the former has been shown to determine SF-1 binding specificity to sumo-sensitive response elements. The basic enzymology behind sumoylation of SF-1 K119 sumoylation is not fully understood nor optimized with the reaction taking well over 8 hours while still not reaching completion. Similarly, sensitive visualization assays are not currently available in order to facilitate kinetic studies of this *in vitro* reaction. This graduate work focuses on sumoylation of the SF-1 DBD with the goal of developing a more robust and sensitive in vitro system in order to assay new potential SF-1 binding sequences and apply the revamped protocol to other sumoylation substrates. Our work demonstrates that the rate-limiting step of the enzymatic reaction is the loading of the E2 enzyme, Ubc9, and pre-loading this enzyme prior to incubation with substrate dramatically enhances the rate of sumoylation. Finally, we attempt to determine how the putative E3 ligase, PIASγ, functions to enhance SF-1 sumoylation *in vitro*.

Table of Contents

Title Page	i
Copyright Page	ii
Acknowledgements	iii
Abstract	v
Table of Contents	vi
List of Figures	vii

Chapter	Page
Introduction	1
Results	7
Discussion	21
Materials and Methods	25
Figures and Legends	30
References	52

List of Figures

	Page
Figure 1: Mouse SF-1 is sumoylated at two sites, K119 and K194	31
Figure 2: SF-1 DBD overpurification	33
Figure 3: In vitro sumoylation optimization	35
Figure 4: Sumoylation affects SF-1 DNA binding	37
Figure 5: The R114Q human mutation does not affect sumoylation of the SF-1 DBD	39
Figure 6: Development of radioactive in vitro sumoylation assays	41
Figure 7: Sumoylation of LRH-1 Hinge-LBD	43
Figure 8: Purification and sumoylation of full-length SF-1	45
Figure 9: PIASγ fragment purification and effects on SF-1 DBD sumoylation	47
Figure 10: Full-length PIASγ purification and activity	49
Figure 11: PIASγ effects on SF-1 sumoylation	51

Introduction

The Nuclear Family

Nuclear hormone receptors (NR) are a large family of ligand-activated transcription factors that play a major role in regulating development, reproduction, immune response, cardiac function, and metabolism (1). NRs are generally defined by an N-terminal DNA-binding domain (DBD), which is composed of two highly conserved zinc-finger motifs, followed by a hinge domain, which confers structural flexibility. The C-terminal region is composed of the ligand-binding domain (LBD), which is a twelve-helix module that binds a receptor's cognate ligand. When inactive, NRs are sequestered in the cytoplasm by heat shock proteins or are bound to DNA regions forming repressive complexes (2). Activating ligands run the gamut of hormones, vitamins, lipids and other intracellular signals. Upon ligand-binding, the structural confirmation of a NR will change resulting in an active state wherein the activated AF-2 domain (Helix-12) will recruit coactivator or corepessor complexes (3). Many NRs form homodimers and heterodimers upon ligand-activation, however some have been found to bind DNA as monomers (4).

Of particular interest to our lab is NR5A1, or Steriodogenic Factor-1 (SF-1), a monomeric member of the adopted orphan receptors. SF-1 has been found to regulate steriodogenic enzymes as well as gonad and endocrine developmental programs (5). An SF-1 knockout mouse exhibited male-to-female sex reversal, died by postnatal day 8, and lacked adrenals, gonads and the ventro-medial hypothalamus (6,7). The SF-1 null mice were also deficient in corticosterone, suggesting that adrenocortical insufficiency was the probable cause of death. In adrenocortical cells, SF-1 increases expression of the

corticotropin receptor (MCR2), STAR (steriodogenic acute regulatory protein), and all of the enzymes required for cortisol or corticosterone biosynthesis (8). SF-1 also increases the expression of many testicular genes required to develop and maintain the male phenotype. In Leydig cells, for example, SF-1 stimulates the LH receptor, STAR, and the CYP11A1 and CYP17 enzymes required for testosterone biosynthesis (9).

Of Forms and Structure

Of the three functional domains of SF-1, only two have been structurally crystallized. The Ftz-F1 domain containing SF-1 DBD (aa1-111) has been visualized by stabilizing the structure with double-stranded (ds) DNA (10). The Ftz-F1 domain is conserved within the NR5A family and forms an α-helical structure at the C-terminal extension, allowing for long-range noncovalent interactions with the core DBD. Although some aromatic Ftz-F1 residues could nonspecifically interact with DNA, the LRH-1 DBD-DNA structure (liver receptor homologue-1, NR5A2) indicates that mutations disrupting the α-helix do not affect DNA-binding affinity (11). Our lab has structurally visualized the LBD of SF-1 and LRH-1, determining that phosphatidyl inositols likely occupy the ligand-binding pocket (12). The presence of such an ubiquitiously available ligand attests to the constitutively active state of SF-1, although modification of the phospholipids head group could modulate SF-1 activity.

Our lab has further shown that post-translational modifications such as phosphorylation and sumoylation play a major role in modulating SF-1 activity (13-15). Mitogen-activated protein kinase phosphorylation (MAPK) of Serine203 on the hinge

domain mediates interaction with coactivator glucocorticoid receptor interacting protein-1 (GRIP1) and corepressor SMRT (silencing mediator of retinoic acid and thyroid hormone receptor) (13). SF-1 sumoylation at sites K119 and K194 has been shown to repress transcriptional activity, while not affecting its cellular localization (14). SF-1 sumoylation is enhanced by PIASxα and PIASγ and mediated by the DEAD-box protein DP103. The sumoylated state of SF-1 determines whether or not it can bind particular DNA response elements, wherein only unsumoylated SF-1 can bind the rat inhibinα sequence. Similarly, SF-1 pre-bound to the high affinity sequence of MIS (Mullerian Inhibiting Substance) can no longer be sumoylated, suggesting a confirmational change in the sumo recognition site upon DNA binding. The aforementioned crystallography studies have so far failed to shed light on how sumoylation structurally affects full-length SF-1 conformation. The published DBD construct ends several amino acids before the K119 site, and while nuclear magnetic resonance (NMR) studies of K194 sumoylation demonstrate that it does not affect LBD orientation, this study included only a small portion of the hinge region (10,15). The localization of the sumoylation sites on the flexible hinge region could result in significant perturbance of the overall structure upon sumo modification.

Our lab has recently shown that a knock-in mouse with an unsumoylatable SF-1 (2KR) results in impaired adrenal and gonadal development, a result of misregulation of a novel subset of SF-1 target genes (Lee et al, submitted). While it had been previously proposed that sumoylation functions to simply repress transcriptional activity, these results indicate that sumoylated SF-1 functions to prevent inappropriate activation of select target genes during development. This *in vivo* analysis provides evidence that

unmodified and sumoylated substrates function differently allowing for increased modulation of SF-1 transcriptional regulation.

The SUMO way

Ubiquitin and the family of ubiquitin-like proteins (Ubls) function to post-translationally modify substrates via covalent attachment to cognate lysines. Sumo (small ubiquitin-like modifier) is distantly related to ubiquitin (~18% aa identity) and was discovered by its covalent attachment to the GTPase activating protein RanGAP1 (16). In vertebrates, three paralogs are expressed, SUMO1, 2 and 3. SUMO2 and SUMO3 differ only in their three N-terminal residues and have yet to be functionally differentiated, while they are 50% identical to SUMO1 (17). Like most Ubl, SUMO1 and SUMO2/3 are translated into a precursor that must be processed in order to reveal the C-terminal glycine residue that is linked to the lysine side chains in target proteins. This is achieved by the sumo-specific protease Ulp1/2 in yeast and Senp1-5 in mammals (18). Sumoylation has been found to play a role in cell cycle progression, genomic integrity, subcellular transport, ubiquitin antagonism and enhancement of protein-protein and protein-DNA interactions (19-23).

Sumoylation is highly analogous to ubiquitination, wherein the E1 protein catalyzes a three-part reaction (22). First, the C-terminal carboxyl group of SUMO1 attacks ATP, forming a SUMO1 C-terminal adenylate. The thiol group of the E1 catalytic cysteine then attacks the SUMO1 adenylate, releasing AMP and generating a high-energy thiolester bond. This activated sumo moiety is then transferred to the sole E2 enzyme, Ubc9, via thiolester bond exchange which in turn sumoylates target proteins. The Ubc9

recognition sequence is composed of ΨKXE sequence, wherein Ψ is a large hydrophobic amino acid, K is the target lysine for modification, X is any amino acid followed by a glutamic acid residue. A patch surrounding the Ubc9 active cysteine directly binds to the ΨKXE sequence. Ubc9 lysine14 in mammals and lysine153 in yeast have been found to be sumo-modified and may play a role in substrate recognition and kinetics, yet beyond the catalytic cysteine93, few other 'catalytic' residues have been found (24).

PIAS and Friends

Similar to the ubiquitination pathway, sumo E3s have been identified and are composed of three main families: PIAS (protein inhibitor of activated STAT) proteins, the RanBP2/Nup358 domain-containing proteins and the polycomb Pc2 proteins (25-27). Previous work in the Ingraham lab demonstrated that PIAS family members not only interact strongly with, but also mediate enhanced sumoylation of SF-1 in cellular assays. There are four PIAS proteins, 1, xα, 3 and γ, which were discovered via PIAS1's repressive effects on STAT1 (signal transducer and activator of transcription)-activated genes (28). PIAS proteins are composed of three main functional domains: an N-terminal SAP (SAF/Acinus/PIAS) domain known to bind AT-rich regions of DNA, a central RING (really interesting new gene) domain known to mediate protein-protein interactions and a C-terminal sumo-interaction motif as well as several potential sumoylation sites (22).

PIAS proteins have been shown to play many roles in numerous cellular pathways. The C-terminal domain of PIAS1 has been shown to strongly interact with the N-terminal region of activated STAT1 while also directly competing with STAT1 for

response element binding (28,29). The C-terminal acidic domain of PIAS3 was required for an interaction with transcriptional coactivator TIF2, while both PIAS1 and PIAS3 have been shown to interact with the TATA-binding protein, alluding to their roles in transcriptional gene regulation (30,31). PIASγ has been shown to repress the LEF1 transcription factor by mediating its relocalization into nuclear bodies, an activity dependent on its RING domain (32). The structural similarity of PIAS proteins to the E3 ubiquitin ligases led many to posit a similar role for sumoylation. In fact, PIAS1 has been shown to kinetically enhance c-Jun and p53 sumoylation while PIASxα has been shown to mediate androgen receptor sumoylation and subsequent repression of transcriptional activity (33,34).

Previous work in the Ingraham lab has shown in a mammalian 2-hybrid assay that PIASγ specifically interact with SF-1 and that a co-transfection of PIASγ with SF-1 results in increased SF-1 sumoylation (14). However, *in vitro* sumoylation (IVS) of SF-1 can be accomplished with only E1, Ubc9 and sumo substrate, raising the question of exactly how PIASγ enhances SF-1 sumoylation.

This graduate work focuses on the enzymology behind SF-1 sumoylation. Beyond optimization of the IVS, we also ask if SF-1 sumoylation could provide mechanistic answers to cellular transcription data. We address if a recently described human mutation could affect SF-1 sumoylation and lastly, attempt to stabilize the hinge region for structural studies.

Results

Steriodogenic Factor-1 is sumoylated at two sites, lysine 119 and lysine 194

SF-1 is a constitutively active nuclear hormone receptor. As a result, the post-translational modifications SF-1 undergoes play an even more important role in its regulation. Within the SF-1 hinge region are two post-translational modifications of particular interest to our lab, sumoylation at sites K119 and K194 (Figure 1A). As seen in Figure 1B, bacterially expressed full-length SF-1 is sumoylated at two sites, as is the Hinge-LBD construct, whereas the SF-1 DBD construct or the LBD construct alone are singly sumoylated. One can also see that of the four SF-1 constructs, the DBD protein is most poorly sumoylated.

SF-1 DBD over-purification and optimization

Achieving complete and efficient sumoylation of the fifty-seven kilodalton (Kd) SF-1 DBD construct was a major component of this graduate work. The first question we addressed was how the substrate could be optimally purified in order to completely sumoylate the protein. The SF-1 DBD construct contains an N-terminal Maltose-Binding protein (MBP), which allowed for amylose bead affinity purification of the protein from bacteria. Upon maltose elution from the beads, the DBD is then subjected to anion chromatography over a HI-trap Q column with eluted fractions coming off at 350mM ammonium acetate and ready for subsequent *in vitro* sumoylation assays (15) (Figure 2A). Across the eluted fractions, no difference was found with respect to increased sumoylation (Figure 2B), so we asked if the purification achieved via anion

chromatography could be accomplished by gel filtration. However, the elution from the amylose beads and subsequent concentration and injection into a Superdex-200 sizing column resulted in the protein coming off as aggregate fractions, as evidenced by the very early elution off the column (Figure 2C). Perplexed, we took the anion fractions, pooled and concentrated the protein and injected it into the sizing column and found that protein now eluted into four main fractions, corresponding to monomer (peak#4~67 kD), dimer (peak #3~144kD), hexamer (peak#2~440kD) and aggregate sizes (peak#1) via sizing column standards (Figure 2D). Visualized by SDS-PAGE gel, these fractions all appear similar, although with varying levels of purity (Figure 2E). We subsequently tested all the fractions, comparing which purification method achieved maximal sumoylation. Surprisingly, the initial affinity purification was the optimal substrate as evidenced by having more slower-migrating su-SF-1 than any of the subsequent purification methods (Figure 2F). Although the amylose-anion-then sizing method appears to have equal sumoylation to the affinity purified substrate, the prolonged purification procedure and reduced yield to obtain equally optimal substrate did not merit the extra work. For subsequent experiments we utilize only MBP affinity-purified SF-1 DBD.

Of Enzymes, Energy and Salts

Previous work in the Ingraham lab performed *in vitro* sumoylation assays (IVS) overnight, at 4° with the following protein concentrations: 140 nM E1, 3.2 μM Ubc9, 24 μM Sumo1 and 2.8 μM SF-1 DBD (Cambell et al, 2008). Although these assay conditions partially sumoylate the DBD, the long incubation period and poor total

sumoylation was always a concern. To address this, we ran an IVS without substrate to determine if Ubc9 was being fully trans-conjugated during the assay. At first, the appearance of a su-Ubc9 moiety above the free sumo band was promising, indicating that Ubc9 was in fact being loaded with a sumo substrate (Figure 3A). However, when performing the same assay with SUMO2, which migrates slower than SUMO1, we found that even after 3 hours at 37°, not all of the Ubc9 was being fully sumo-conjugated. With the realization that the likely bottleneck in the reaction was not sumoylation of the SF-1 DBD substrate, but rather the trans-conjugation step of E1-sumo transfer to Ubc9, we decided to increase the Ubc9 concentration from 3.2 μM to 5 μM, and reduce the SF-1 DBD concentration to 1 μM, such that it would be the limiting reagent in the reaction. We also determined that 20 μM of sumo was sufficient to maintain an excess of sumo substrate (Figure 3B). All subsequent assays are performed with 140 nM E1, 5 μM Ubc9, 20 μM sumo and 1 μM SF-1 substrate.

During a joint lab meeting with the Morgan lab it was demonstrated that during an ubiquitination assay, prior to incubating the machinery with substrate, they would pre-load their enzymes by incubating machinery, ATP and ubiquitin alone for 15'. We attempted this pre-loading step with the re-worked IVS assay and found that it greatly increased the rate of our sumo reactions. As seen in Figure 3C, pre-loading the machinery for 15' and subsequent addition of the SF-1 substrate results in at least 50% of the substrate being sumoylated within the first 10' whereas lack of pre-loading took one hour before 50% sumoylation occurred. The improvement in sumoylation rates held true even when using SUMO2 (Figure 3D) or if we used a different substrate, as shown in Figure 3E with SF-1 LBD.

Since the DBD construct only contained the K119 sumo site, another concern during IVS was the appearance of a second sumoylated band during reactions, as evidenced by the slower migrating band above 1xsumo SF-1 band. Using the K119A DBD mutant, we show that this is a minor component of the overall sumoylated product, and is likely the result of the *in vitro* nature of our assay (Figure 3F). We attempted to overcome this problem by mutagenizing other potential lysines in the DBD construct, but found that most ideal lysine substrates predicted by the SUMOplot program (REF) lay within the highly conserved FTZ-F1 domain (K100, K106). In fact, though K106R showed reduced but not total loss of cryptic sumoylation, the mutant DBD resulted in a dramatic loss of SF-1 binding abilities to known SF-1 binding sequences (results not shown). As a result, the SF-1 DBD construct was left as such for all successive assays.

The final component of the IVS assay we addressed was the buffer. Previous work in our lab performed IVS assays in 50mM Tris-HCl, pH 8, 100mM NaCl, 10mM MgCl2, 2mM ATP and 0.2 mM DTT. We attempted several ATP variations from increasing the amount of ATP in the reaction to including an ATP regenerator system but found the freshness of the ATP to be the most critical. The Lima group also published a paper that utilized an entirely different buffer composed of: 20mM Hepes pH 7.5, 50mM NaCl, 5mM MgCl2, 0.2mM DTT and 1mM ATP, which when compared with our current buffer resulted in a dramatic improvement of sumoylation (35) (Figure 3G). Description of the radioactive assay shown in this figure will be discussed in a later section. All successive assays have been performed with the Hepes buffer.

The Protein and the DNA

Previous work in the lab has shown that sumoylated SF-1 selectively binds known SF-1 target sequences (15). Campbell et al showed that su-SF-1 could bind a double-stranded (ds), 51 basepair (bp) oligo containing the high affinity site of hCYP11A regardless of its sumoylated state, whereas only unsumoylated SF-1 can bind the low affinity site of Inhibin-alpha. A recently submitted paper by Lee et al demonstrates that a knock-in of an unsumoylatable version of SF-1 into a mouse model led to misregulation of novel SF-1 target genes. Among the misregulated genes was Sonic Hedgehog (SHH), which contains six potential SF-1 binding sites, and mAkr1c18 the mouse homolog of hAKR1C1. In order to determine if these were bona fide SF-1 binding sequences and whether they were sumo-sensitive, we generated 51 bp oligos containing the proposed SF-1 response elements (RE) (Figure 4A) and tested them in an electrophoretic mobility shift assay (EMSA). As seen in Figure 4B, hAKR1C1, mAkr1c18 (which contain the same SF-1 RE) as well as mSHH binding site (bs) #1 are not only true SF-1 RE's, but are also sumo-sensitive in that only the un-sumoylated form of SF-1 can bind the oligos. This is in contrast to hCYP11A1, which can be bound by either the sumoylated or unsumoylated forms of SF-1 DBD. However, another potential response element, Nurr77 site #2, is not an actual SF-1 binding site.

mSHH contains six putative SF-1 RE, and Figure 4C demonstrates that all of these are true SF-1 binding sites, although the DBD's affinity differs from sequence to sequence. Of the identified mSHH sites, only bs#2 is not sumo-sensitive, as evidenced by the strong binding of sumoylated SF-1. Curiously, there is also a higher migrating band present in mSHH bs#5 (Figure 4B and 4C), however this is likely not K119-

sumoylated SF-1. Since the DBD construct can be doubly-sumoylated, the su-SF-1 moiety binding mSHH bs#5 is likely sumoylated at another site and is an artifact of the IVS reaction. This is supported by the K119A DBD mutant strongly binding the mSHH bs#5 only when it is unsumoylated and likely appears only with bs#5 due to SF-1's high affinity for this site. In fact, this cryptically sumoylated SF-1 DBD explains the slowest migrating band in the hCYP11A1 and mSHH#2 lanes.

Does the R114Q mutation affect SF-1 sumoylation?

SF-1 deletion in mice has been shown to affect gonadal and adrenal development, as well as male to female sex reversal in mice (36). Human mutations in SF-1 have been shown to result in adrenal failure, XY reversal and XY primary amenorrhea. Thus when a human mutation was mapped to R114Q and resulted in vanishing testes, we wanted to ask whether or not the proximity of this mutation to the K119 sumoylation site had any effect on the sumoylation of the SF-1 DBD. Although the recognition sequence for UBC9 sumoylation of substrates is largely limited to the ΨKXE sequence, it is possible that the R114Q mutation could affect the rate of SF-1 sumoylation.

As shown in Figure 5A, a timecourse of SF-1 DBD sumoylation versus the R114Q mutant did appear to sumoylate slightly slower than wildtype with SUMO1, although given enough time, eventually reached fully-sumoylated status after three hours. Similarly, sumoylation of WT SF-1 versus R114Q with SUMO2 showed no major difference (Figure 5B). Interestingly, the rates of SF-1 sumoylation for SUMO1 versus SUMO2 for these experiments were dramatically different. Comparing the WT panel for SUMO1 versus SUMO2, one can see that full sumoylation with SUMO1 takes at least

~45', whereas the DBD can be fully-SUMO2ylated within five minutes post incubation of the substrate with pre-loaded machinery. This could be the result of the presence of sumo-interaction motif (SIM) domain within the DBD construct specific to SUMO2 (Zhu et al 2008). These experiments differ from Figure3C and D in that they utilize the optimized Hepes buffer.

Another assay our lab uses to assess SF-1 DBD activity is its inability to be sumoylated while bound to known SF-1 binding sequences (LC). As shown in Figure 5D, the R114Q mutant was equally reduced in terms of sumoylation when pre-bound to the high affinity double-stranded (ds) binding sequence of Mullerian Inhibiting Substance (MIS). Lastly, SF-1 and R114Q, after being sumoylated, similarly bound or failed to bind known SF-1 binding sequences, as mentioned in the previous section (Figure 4C). As a result, we conclude that the R114Q human mutation phenotype cannot be explained by a sumoylation defect, as it neither affects rate of sumoylation nor the binding properties of sumoylated SF-1.

Radioactive *in vitro* sumoylation assay

Alongside optimization of the IVS, which is then visualized via coommassie staining, we undertook the development of a radioactive sumo assay to better quantitate our results. Our initial attempt involved using the Promega TNT system, using ^{35}S–labeled methionine to label the *in vitro* transcribed/translated (IVTT) sumo substrate. As seen in lane 1, Figure 6A, IVTT SUMO1 results in a primary band running at the expected size of 12 kD. However, a much higher running band also appears, which can be collapsed when the reaction is treated with sumo protease Ulp1 (18). This band may

be the result of trace sumoylation machinery present in the rabbit reticulocyte lysate, resulting in sumoylation of RanGAP or another prominent substrate (37). Nevertheless, 30' treatment of the IVTT reaction with Ulp1 sumo protease results in complete collapse of the band. However, the introduction of Ulp1 into the reaction could conceivably skew any future uses of the sumo substrate. Therefore IVTT reaction was subsequerntly bound onto TALON nickel beads and washed to remove the Ulp1 protease and any nuclear contaminants. His-tagged SUMO1 is then cleaved off the beads via TEV incubation, resulting in free ^{35}S labeled SUMO1. Although TEV cleavage successfully removes a majority of the sumo substrate from the beads, a residual amount is left on the beads, as evidenced by the hot SUMO1 bands eluting from the beads after imidazole elution (Figure 6A).

An advantage of radioactive IVS is increased sensitivity of our reactions. Thus we scaled down the aforementioned reactions ten-fold and used 8 μL of radioactive sumo per reaction (each IVTT and subsequent purification process yielded 80μL of radioactive sumo). As shown in Figure 6B, the scaled down reaction resulted in single and double (cryptic) sumoylation of the SF-1 DBD with radioactive SUMO1 and 2, which could now be quantitatively followed over time. However, generating a radioactive substrate in this manner had two major drawbacks: 1) due to the IVTT and purification steps, we were never completely sure how much hot sumo is added to each reaction, relying only on volume added per reaction and 2) the IVS reactions contained bacterially-produced cold sumo whereas the radioactive sumo was generated from mammalian reticulocyte lysate. Although theoretically similar, we could never say that the hot and cold components were the same.

In order to address this, we utilized a ^{32}P labeling system developed by the Morgan lab. This system places ubiquitin (or in our case the sumo) substrate into a vector, behind an N-terminal glutathione sepharose tag (GST)-TEV protease site and protein kinase A (PKA) sequence. As seen in figure 6C, the GST-tagged construct is easily labeled by PKA using ^{32}P-gamma labeled ATP as our donor. Following a spin step that removes free ^{32}P -ATP and a subsequent TEV cleavage step for 3 hours, the ^{32}P -labeled sumo moiety can then purified out of the TEV/GST mixture by incubation at 65° for 15', five minutes on ice and a 15' high speed spin at 13,000 rpm. Remarkably, as in the case of ubiquitin, the sumo protein is stable enough that it is the only protein to remain soluble, with all other components of the cleavage reaction precipitating out of solution into a pellet during the spin. This is better demonstrated by Figure 6D, wherein a cold version of this reaction shows that only the sumo protein is recovered after the purification step. The true value of this method lies in that we could now generate completely identical radiolabeled and cold substrate. For use in ^{32}P-sumo IVS reactions, protein concentrations are reduced ten-fold, wherein 1μM of hot sumo is added to 1μM of cold sumo, allowing for quantitative IVS reactions (Figure 6E).

LRH-1/Beta-catenin structure and sumoylation

Through collaborating with Dr. Fumiaki Yumoto in the Fletterick lab, we learned that co-expression of the Hinge-LBD construct of LRH-1 with β-catenin led to the formation of a stable complex (38). The proteins interacted so stably with one another that mixing individually purified LRH-1 and β-catenin, and subsequent purification through a gel filtration column led to a stable complex. Since the Hinge-LBD LRH-1

construct contained the primary K270 sumo site (39), we wanted to ask, does the stable formation of this complex affect sumoylation of the LRH-1 protein? As seen in figure 8A, a time course experiment comparing the rate of sumoylation between LRH-1 hinge-LBD alone, LRH-1-β-catenin preformed complex, and LRH-1-β-catenin gel-filtered complex; there does not appear to be any major differences in terms of sumoylation rate. Even with overnight IVS reactions, the LRH-1-Hinge-LBD construct is sumoylated to a maximum of about 70% with the presence or the absence of β-catenin having little effect. This concluded our foray into the LRH-1-β-catenin complex and structure formation.

Purification and sumoylation of full-length SF-1

In vitro studies of SF-1 predominantly involve either the N-terminal region containing the DBD or C-terminal constructs composed of the hinge and LBD. Production of full-length SF-1 has been hampered folding and solubility problems. However, Dr. Yumoto found that by growing BL-21 bacteria induced with very low amounts of IPTG (isopropyl β-D-1-thiogalactopyranoside) for 22-24 hours at 16° leads to sufficient production of full-length SF-1. The critical components of the purification process were speed and binding of the eluted fractions to a 12-mer ds oligo of hCYP7A (Figure 7B). The purification procedure is done as quickly as possible, with a single, two minute sonication, 45’ spin at 15000g, 30’ binding of the lysate to beads, 30’ washing of the beads, and very quick elution from the beads directly onto ds hCYP7A oligo. After a 30’ incubation at 4° with the oligo, the sample is then concentrated to a 1 mL total volume and injected into a sizing column to separate the stabilized DNA-bound SF-1 from aggregates and free DNA dimers (Figure 7A). The purified protein runs at about 57

kDa and is sumoylated at similar rates with SUMO1 and SUMO2. Interestingly, the rapid rate of sumoylation seen with SUMO2 and SF-1 DBD (Figure 5B) does not occur with full-length SF-1. In order to determine which site was being sumoylated faster, K119 or K194, full-length SF-1 was incubated overnight with 51 bp ds oligo, in an attempt to displace the much smaller 12 mer hCYP7A oligo. Replacement with a much longer oligo led to reduced sumoylation of the second site, while the overall rapid sumoylation of the first site was unaffected, implying that the K194 site is the first site to be sumoylated, as addition of the longer oligo did not affect its rapid rate of sumoylation (Figure 7D). While structural studies are ongoing, we are also utilizing this protein with second generation MITOMI devices in an attempt to map all possible SF-1 binding sequences (40).

PIASγ, the Odγsseγ

Previous work in the Ingraham lab demonstrated that when pre-bound to a high affinity site like MIS, the SF-1 DBD could no longer be sumoylated (Figure 9C). Coupled with the unclear role of PIASγ in enhancing SF-1 sumoylation, this posited an ideal situation to test if PIASγ enhancement SF-1 sumoylation lay in mediating sumoylation of DNA-bound SF-1.

Initial attempts at purifying full-length PIASγ from bacteria proved very difficult. Despite numerous changes to induction times and concentrations, different purification tags and visibly induced PIASγ bands on gels, solubility remained the fundamental problem. In order to circumvent this problem, we obtained fragments of PIASγ from the Sui group of Wake Forest University (41). As shown in Figure 9A, the designed fragments largely cover the entire protein, allowing for purification of individual

functional domains like the Saf/Acinus/Pias (SAP) domain, Siz1/PIAS-RING zinc finger domain and a putative sumo-interaction motif (SIM). All of the fragments were easily expressed and found to be in the soluble fraction post bacterial lysis.

The first question we asked with these fragments was what effect they had on DBD sumoylation. As seen in Figure 9B, SF-1 can be sumoylated to high levels as indicated by the two slower migrating bands above unsumoylated SF-1. However increasing amounts of GST, GST-tagged 1-323, 266-468 and 324-507, specifically around [7.5 μM], began to decrease SF-1 sumoylation levels. This served as a general inhibitory concentration among all the proteins tested. However, the endpoint design of this experiment was flawed in since SF-1 was already maximally sumoylated, thus, if these fragments did have an effect on the rate of sumoylation, the reaction would not display any difference.

In order to better address whether or not sumoylation of SF-1 was affected by the addition of these PIASγ fragments, we designed time-course experiments with or without addition of ds MIS oligo. All PIASγ fragments and the GST negative control were added at 3 μM and as shown in Figure 9C, the addition at this concentration of protein did not inhibit nor enhance the overall rate of sumoylation. However, if SF-1 DBD is pre-incubated with ds MIS oligo, as seen in the control panel, no appreciable sumoylation of the DBD occurs. The remaining panels demonstrate that the addition of any fragment of PIASγ does not alleviate DNA-binding mediated repression of sumoylation.

Drum Roll Please…

Due to the negative results from using PIASγ fragments, we resolved to purify full-length PIASγ from mammalian cells. Using our FLP-FRT inducible system in HEK 293 cells, we flag-tagged full-length SF-1 and generated a tet-inducible, stably expressing cell line. Figure 10A is an immunocytochemistry staining of nuclear label DAPI which co-localizes with 3x-flag-tagged PIASγ. PIASγ expression was uniformly nuclear with occasional nuclear puncta staining, commensurate with previously published work (14). In order to purify PIASγ from mammalian cells, we modified a nuclear preparation protocol developed by the Spiegelman group and coupled it to FLAG based purification scheme from the Morohashi group (42,43). From 8 x 15cm dishes of confluent tet-induced HEK 293 cells, we recovered roughly 250 μg of PIASγ. As shown in Figure 10B a single flag-reactive band is found in each of the isolated lanes. Despite losing over half of the flag-tagged product during the hypertonic supernatant and pellet separation, the coommassie gel still shows a single, purified band indicating decent recovery of full-length PIASγ.

The first question we asked was whether or not PIASγ was functional. Previous work by the Lima group showed that PCNA sumoylation at lysine164 was PIASγ-dependent, while lysine127 sumoylation occurs independently (35). Using a K127R mutant, Figure 10C demonstrates that PCNA K164 can be *in vitro* sumoylated in a PIASγ dependent manner. Knowing we purified functional PIASγ, we next tested how it affects full-length SF-1 sumoylation in our radioactive assay with radiolabeled SUMO1 and SUMO2. Since the radioactive assay uses much less protein than the previous coommassie assay, we performed the IVS with increasing amounts of PIASγ to determine

the optimal concentration for activity. Surprisingly, we found that increasing amounts of PIASγ led to slightly reduced levels of SUMO1-SF-1 (Figure 11A). However the appearance of a sumoylated PIASγ band could explain the reduction in su-SF-1 as two substrates were now consuming the radiolabeled Sumo. Thus we tested the rate of SF-1 sumoylation at 100nM PIASγ, a concentration that did not result in the appearance of sumoylated PIASγ. As seen in Figure 11B, in the absence of PIASγ, SF-1 becomes sumoylated at the 15' mark, however with the addition of PIASγ, su1-SF1 does not appear until the 30' mark, indicating that the addition of PIASγ resulted in reduced SF-1 sumoylation. Since full-length SF-1 is stabilized by a 12-mer hCYP7A ds oligo, it was suggested that perhaps the presence of this DNA element impaired SF-1 sumoylation. In order to test this hypothesis, equal amounts of SF-1 bound to DNA, free SF-1 and free SF-1 incubated with PIASγ were sumoylated. As Figure 11C exhibits, the absence of the hCYP7A ds oligo led to a loss of soluble SF-1 (evidenced as well by a precipitated residue present in the reaction tube) and as such, a reduction in the amount of sumoylated SF-1. With a proverbial poke in the eye, the addition of PIASγ to this reaction led to reduced sumoylation of the SF-1 protein that remained in solution. This result is the same whether SUMO1 or SUMO2 is utilized.

In our final experiment with full-length PIASγ, we asked whether or not addition of PIASγ overcame the inhibition of sumoylation mediated by DNA. Full-length SF-1 was pre-incubated with ds MIS oligo (in order to displace the 12mer hCYP7A oligo), and further incubated overnight at 4° with the IVS reaction. As seen in Figure 11D, the presence of MIS oligo led to an overall reduction in sumoylated SF-1 levels, while the addition of PIASγ to MIS bound SF-1 failed to rescue the inhibition of sumoylation.

Discussion

The SF-1 DBD is a relatively stable and soluble bacterially-produced substrate. The published DBD purification protocol involved an anion chromatography step post maltose elution. This purification step served to remove remaining contaminants in the eluate yet also reduced levels of DBD sumoylation (Figure 2F). Given the nature of an anion column, wherein quaternary ammonium particles are bound to agarose beads, it is likely that such exposure led to misfolding of the DBD and as a result reduced surface exposure of the K119 site. This misfolding can be reversed upon elution from a gel filtration column where the separation of aggregated, misfolded particles allowed the soluble and folded SF-1 to be sumoylated. It is intriguing that maltose eluted DBD is initially in the aggregate fraction, yet can be sufficiently sumoylated. The best we can say is, it works.

Basic enzymology dictates that the rate of any multi-step reaction is determined by the rate-limiting reaction. Although we initially suspected that the DBD was insufficiently pure to achieve maximal sumoylation, realizing that Ubc9 was poorly trans-conjugated with SUMO2 led us, instead, to reconfigure our IVS recipe. Yet increasing the amount of Ubc9 was not the only determining factor as we also found that by pre-incubating Ubc9 with E1, sumo, salts and ATP that the rate of SF-1 sumoylation dramatically increased (44). Previous work by the Pichler group demonstrated that mammalian Ubc9 can be sumoylated at K14 and that this modification affects its substrate specificity (24). How would a K14R mutant perform under similar conditions? Perhaps the improvement in sumoylation lies only in having over 1μM of Su~Ubc9

(charged sumo moiety) upon addition of 1μM substrate; yet it is interesting to speculate that SF-1 DBD may be similar to Sp100, wherein Su-Ubc9~Su recognizes the DBD K119 sumoylation site better.

One mechanism by which su-Ubc9 enhances sumoylation is via sumo interaction motifs (SIM). It is thought that SIMs enhance sumoylation by facilitating interactions with the sumo moiety on Ubc9, resulting in increased local concentration of E2 enzyme in the vicinity of target proteins (45-48). In the case of Bloom syndrome protein (BLM), several hydrophobic residues along a 21 amino acid stretch not only increased sumoylation but also led to a preference for SUMO2 modification over SUMO1. Once the IVS assay was fully optimized, we found that SUMO2 rapidly modified the SF-1 DBD compared to SUMO1 (Figure 5A, B), while finding no such difference with the LBD domain (data not shown). Interestingly, when comparing SUMO1 versus SUMO2 rates with the full-length SF-1 protein, the rates appeared identical (Figure 8C). This discrepancy may be explained by a SIM for SUMO2 visible in the DBD construct alone, yet masked when utilizing full-length SF-1. While there are no obvious similarities between the BLM SIM and the DBD sequence, SIM sequences are vaguely defined and interaction appears to rely more on a structural motif, as opposed to a defined amino acid sequence (47,49).

Structural studies of the NR5 family of transcription factors have successfully visualized the DBD and LBD of SF-1 and LRH-1 (10-12,50). However, the hinge region has remained elusive due to its flexible nature. Our collaboration with Dr. Yumoto aimed not only at determining if β-catenin affected LRH-1 LBD sumoylation, but also whether or not sumoylation of the hinge region would allow stabilization and subsequent

visualization via X-ray crystallography. However the inability to obtain fully-sumoylated protein hindered this project. Despite prolonged incubation periods with sumoylation machinery we could never fully-sumoylate the LRH-1 protein. We attempted to separate sumoylated and unsumoylated LRH-1 by gel filtration but found the two species closely migrated together thereby making a pure isolate difficult. These experiments, however, were conducted before the fully optimized IVS. Perhaps under our revised conditions we can now fully-sumoylate LRH-1.

PIAS proteins were originally thought to be E3 ligases due to their similarity to Ub E3 proteins (35,51,52). Of the four PIAS proteins: 1, 3, Xα/β, and γ, our lab has shown *in vivo* that PIASγ most increased SF-1 sumoylation. Lee et al published that PIASγ co-transfection resulted in increased SF-1 sumoylation while an unpublished mammalian two-hybrid assay found a direct and specific interaction between SF-1 and PIASγ (14,53). Given these data, we hypothesized that purified PIASγ would enhance SF-1 sumoylation *in vitro* and potentially overcome the DNA-mediated inhibition Campbell et al described (15). Yet our results with mammalian, purified PIASγ were completely unexpected. PIASγ failed to enhance SF-1 sumoylation, instead having the opposite effect of reducing total levels of sumoylation. The addition of PIASγ also failed to overcome the inhibition of sumoylation mediated by DNA. How then to reconcile our cellular data with these *in vitro* results? PIAS proteins have been shown to mediate regulation of downstream genes in numerous ways (54-56). Perhaps the enhancement of cellular sumoylation is the result of PIASγ preventing desumoylation of SF-1. PIAS1 has been shown to compete with activated signal transducer and activator of transcription factor 1 (STAT1) for DNA response elements (28,31). PIASγ may function in a similar

manner whereby free SF-1 is subsequently sumoylated since its DNA response elements are occupied by PIASγ. But the simplest explanation of our results is that cellular PIASγ recruits a cofactor that enhances SF-1 sumoylation, a situation our IVS fails to recapitulate. While unpublished work by Dr. Lee has shown that *in vitro* transcribed/translated PIASγ can enhance SF-1 sumoylation, this protein is in the presence of rabbit reticulocyte lysate, thus only proving its necessity, not sufficiency. Dr. Lee has also shown DEAD-box protein DP103 plays a role in PIASγ-mediated enhancement of SF-1 sumoylation yet attempts to purify this protein from bacteria also proved very difficult. PIAS3 has also been shown to enhance SF-1 sumoylation, and could possibly be sufficient *in vitro* (14).

SF-1 sumoylation is proving to be an important post-translational modification whose effects include altered DNA-binding specificity and differential co-factor recruitment (57). Understanding the mechanism of SF-1 sumoylation has led to a clearer view of how this modification contributes to downstream regulation of SF-1 targets. This work has focused on the basic enzymology behind SF-1 sumoylation and aimed to address the role of PIASγ in the reaction. Although the latter was unsuccessful, the author hopes that the work contained in this thesis will serve as a reminder that in graduate school, negative data is still data.

Materials and Methods

Plasmids and Constructs – Mouse SF-1 fragment containing SF-1 LBD (amino acids [aa] 178 to 462, cysteine mutant, described previously (8) was cloned using BamHI-XhoI sites into the bacterial expression vector pBH4 (modified pET-based vector, wherein the his tag is followed by a TEV cleavage sequence) (Clontech). For maltose-binding protein (MBP) fusion proteins, mouse SF-1 full length (aa 1 to 462), Hinge-LBD (aa 106 to 462), and DBD (aa 1 to 122) forms were cloned into the pMALp2X vector (New England Biolabs) modified to contain N-terminal tobacco etch virus protease cleavage site using EcoRI/XbaI (full-length SF-1), EcoRI-HindIII (Hinge-LBD), and EcoRI (DBD) sites. Recombinant His6- Human E1 (SAE1/SAE2), Human SUMO1 (aa 1 to 97) and mouse Ubc9 (aa 1 to 158) were cloned into the bacterial expression vector pBH4 using BamHI-XhoI sites. K119A and K106R point mutants were created using pMAL-SF-1 DBD as a template by PCR mutagenesis (QuikChange site-directed mutagenesis kit; Stratagene). Full-length His-tagged SF-1, LRH-1 Hinge-LBD, and β-catenin in the pRSF1 vector were all kind gifts from Dr. Yumoto of the Fletterick lab while GST-tagged PIASγ fragments (aa1-100), (aa1-323), (266-468), (324-507) were kind gifts from Dr. Sui of Wake Forest University. 3xFlag-tagged PIASγ was pcr amplified from a GST vector with EcoR1/Xho1 ends and subcloned into pcDNA5-frt/TO vector. GST-tagged-PKA SUMO1/2 were generated by subcloning from the pBH4 vector via BamH1/Xho1 sites into the pRDB175 (R. Deshaies) aka pJBS069 (D. Morgan). PCNA (pol30) was a kind gift from the Morgan lab with the K127R mutant generated by QuickChange. All DNA

concentrations were measured by using a spectrophotometer (NanoDrop Technologies), and the validity of the constructs was verified by DNA sequencing.

Cell Culture and immunofluorescence– The PIASγ stable cell line was generated by introducing the Flp-in T-Rex system was into HEK 293 cells cultured in DMEM (Invitrogen), 10% screened FBS (Hyclone), 1% pen-strep by selection and selected with 5 μg/mL Blasticidin and 250 μg/mL Hygromycin (Invitrogen). Cells were induced at ~75% confluency, with 50 ng/mL tetracycline (Teknova) and harvested 48 hours post induction. Immunofluorescence was conducted with primary mouse anti-FLAG M2 antibody, then stained with secondary Alexa 488 rabbit anti-mouse and imaged via Leica inverted fluorescent microscope.

Expression and Purification of proteins – mUbc9, PCNA, and SUMO1/2 (either His- or GST- tagged) were grown by lawn inoculating 1L cultures of LB (Amp) with two plates of O/N grown bacteria, incubated at 37° until an O.D. of 0.4-0.7, then induced to a final concentration of 0.35 mM IPTG for 5 hours at 22°. Both are lysed and purified via TALON beads (Clontech) in 50mM Tris-HCl pH8, 150 mM NaCl, 5% glycerol and eluted with 300 mM imidazole. mUbc9 is then subjected to HiTrap Q chromatography with Buffer A 20 mM Hepes pH 7.5, 2 mM CHAPS, and Buffer B 1 M Ammonium Acetate. mLRH-1 Hinge-LBD, β-catening and Complex were inoculated similarly but in LB (Kan), grown until O.D. 0.8-1.0, then induced with 0.050 mM IPTG and grown 22-24 hours at 16°. Cells were lysed and purified in Buffer A 20 mM Tris-HCl pH8, 1mM CHAPS, 10% glycerol, 5 mM β-mercaptoethanol (β-ME), 20 mM imidazole, 300 mM

NaCl and eluted from TALON beads with 400 mM imidazole. Eluate is then mixed with 1 mL aliquot of TEV protease and dialysed O/N in Buffer B, 20 mM Tris-HCl pH8, 1mM CHAPS, 10% glycerol, 5 mM dithiothreitol (DTT) (TEV is a Cys protease), 200 mM NaCl. Sample is then diluted 5fold with Buffer A then repurified with TALON beads to remove TEV and concentrated to 1 mL. Sample is then Gel Filtered using Superdex 200 10/30 with Buffer C, 20 mM Tris-HCl pH8, 1 mM CHAPS, 10% glycerol, 10 mM DTT, 150 mM NaCl. Full length SF-1 was grown and induced in the same manner as LRH-1 hinge-LBD, but was lysed with 20 mM Tris-HCl pH8, 300 mM NaCl, 5 mM β-ME, 10% glycerol, 20 mM imidazole, eluted from TALON beads with 300 mM imidazole into a tube containing annealed hCYP7A oligo. 1 mM of oligo are annealed in 10 mM Tris-HCl pH 7.5, 50 mM NaCl, melted at 95°, then cooled to room temperature while in a 75° water bath. Oligo-bound eluate is then concentrated to 1 mL then injected into Superdex 75 16/30 with 20 mM Tris-HCl pH8, 1 mM DTT, 10 % glycerol. SF-1 DBD is purified as previously published (8) but no longer includes the anion HiTrapQ step. PIASγ fragments were inoculated in a similar manner, grown to an O.D. of 0.4-0.7 then induced to a final concentration of 0.35 mM IPTG then lysed and purified in 20 mM Hepes pH 7.5, 100 mM NaCl, 5 mM $MgCl_2$ 0.2 mM DTT, 10% glycerol and eluted with 10 mM glutathione. Mammalian full-length PIASγ is purified from 8x 15cm dishes of confluent HEK293 cells, homogenized in hypotonic solution 10 mM Hepes pH7.9, 10 mM Kcl, 1.5 mM $MgCl_2$, 0.5 mM DTT, spun, harvest nuclei then resuspend in hypertonic solution 20 mM Hepes pH7.9, 400 mM NaCl, 1.5 mM $MgCl_2$, 0.2 mM EDTA, 20% glycerol, 0.5 mM DTT, spun down, with the supernatant then dialyzed into 20 mM tris-HCl pH8, 200 mM Kcl, 5mM $MgCl_2$, 10% glycerol, 0.1% Tween-20, then bound to FLAG M2-conjugated

agarose beads for one hour. Bound beads were then washed with 20 mM Tris-HCl pH8, 100 mM KCl, 5 mM $MgCl_2$, 10% glycerol, 0.1% Tween-20. PIASγ is then eluted with 0.16 mg/mL 3x FLAG peptide in 50 mM Tris-HCl pH8, 100 mM KCl, 5 mM $MgCl_2$, 10% glycerol, 0.1% Tween-20. All lysis buffers and homogenization buffers contain 1 tablet of Roche Protease inhibitor cocktail.

In vitro sumoylation assays - SF-1 in vitro sumoylation (IVS) assays were carried out in 50 μL reactions with 1 μM SF-1 DBD, 0.12 μM E1, 4 μM Ubc9, and 20 μM SUMO1 in a sumoylation buffer containing 50 mM Tris-Hcl (pH 8.0), 100 mM NaCl, 10mM MgCl2, 2mM ATP, and 2 μM DTT at 37° for 1.5 hours or 20mM Hepes pH 7.5, 50mM NaCl, 5mM MgCl2, 0.2mM DTT and 1mM ATP. Reactions were then resolved by 7.5% sodium dodecyl sulfate polyacrylamide gel electrophoresis (SDS-PAGE) and visualized by Coommassie blue staining. DNA inhibition assays followed the same protocol but involved incubation of SF-1 DBD with ds MIS oligo for 30 min prior to sumoylation reaction.

Electrophoretic mobility shift assays - (EMSAs) were performed by completing an IVS assay then adding 2 mM DTT, and 10 μM double-stranded oligonucleotides of SF-1 target gene promoters. The reaction was then split in half, of which one had 3units Ulp1 protease added (Lifesensors) and both incubated at room temperature for 30 minutes. 12 μL of each sample was then run on an SDS-PAGE for total protein with the other 12 μL loaded onto a 6% native polyacrylamide gel and electrophoresis was carried out in 1x

TBE buffer at 4°. The native gel was analyzed using a fluorescence-based EMSA kit (Molecular Probes) and visualized on a Typhoon laser scanner @ 488 nM.

Radioactive SUMO1/2 labeling – For ^{35}S assays, manufacturers instructions were followed for the Promega TNT Transcription/Translation system (L1170). Post incubation, lysate was incubated with 10units of Ulp1 protease (Lifesensors) for another 30 min, bound onto TALON beads, washed with mUbc9 lysis buffer, then incubated with TEV protease for 1 hour at 4° and with collected flowthrough containing the labeled sumo moiety. For ^{32}P assays, GST- purified SUMO1/2 is incubated with 1 μL crude ^{32}P, 30 μg protein, 2 μL PKA, 5 μL PKA buffer and 1μL 1 mM ATP for one hour at 30°, then subjected to a G-25 column (GE Healthcare), then incubated with 5 μL TEV, 7 μL 10x TEV buffer (200 mM Tris-HCl pH8, 1.5 M NaCl, 10 mM CHAPS, 20 mM DTT) and incubated for 3 hours at 30°. Sample is then heated to 65° for 15 minutes, ice for 5 minutes and spun down at 15000 rpm for 15 minutes.

Figures and Legends:

Figure 1: Mouse SF-1 is sumoylated at two sites, K119 and K194. (A) A schematic of SF-1 constructs describing functional domains and location of the two sumoylation sites. (B) In vitro sumoylation assays, coommassie-stained. The first lane depicts unmodified substrate, while the third lane demonstrates SUMO1 modified substrate and the second lane, the effects of Ulp1 Sumo protease (10 μL in vitro reactions). SF-1, unmodified SF-1; suSF-1, singly sumoylated SF-1; 2xsu-SF-1, doubly sumoylated SF-1; su-Ubc9, sumoylated Ubc9. Asterisk denotes wild-type SF-1 degradation product.

Figure 1

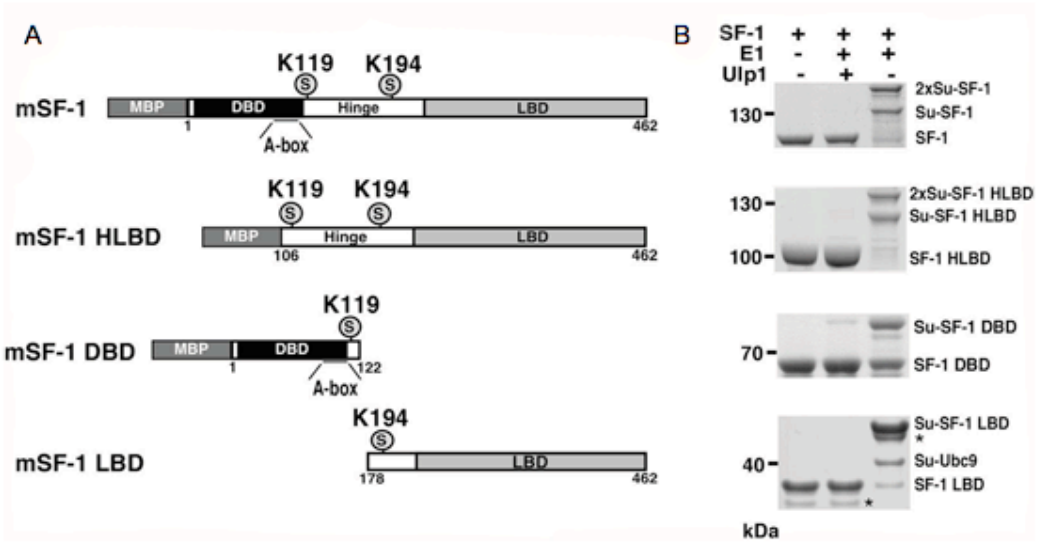
A
K119
K194
mSF-1
MBP
DBD
Hinge
LBD
1
462
A-box
mSF-1 HLBD
106
mSF-1 DBD
122
mSF-1 LBD
178
B
SF-1
E1
Ulp1
2xSu-SF-1
Su-SF-1
SF-1
130
2xSu-SF-1 HLBD
Su-SF-1 HLBD
SF-1 HLBD
100
Su-SF-1 DBD
70
SF-1 DBD
Su-SF-1 LBD
Su-Ubc9
SF-1 LBD
40
kDa

Figure 2: SF-1 DBD overpurification. (A) FPLC trace of a HiTrap Q chromatography of affinity purified DBD. Protein (blue line) was loaded with Anion Buffer A and eluted with a gradient of Buffer B (Buffer A + 1M Ammonium Acetate, brown line). Y-axis is in mAU, which corresponds to the A260 measurement of elutions, X-axis is in volume. (B) IVS of individual eluted fractions from the HiTrapQ chromatography (60 μL reactions) visualized via Coommassie staining. (C) Gel filtration trace of Superdex 200 16/60 chromatography with affinity purifed DBD. Protein was loaded with Maltose lysis buffer. (D) Gel filtration trace of HitrapQ fractions #32-35. Protein was loaded with Anion Buffer A + 350mM Ammonium acetate, the calculated concentration at which DBD eluted from the HiTrap Q. Peak numbers correspond to 1) Aggregates, 2) Hexamers, 3) Dimers and, 4) Monomers of SF-1(E) SDS visualization of lysed and purified SF-1 DBD fractions, Coommassie stained. (F) Triplicate IVS reactions of purified DBD fractions (60 μL reactions), Coommassie stained. Protein concentrations were 140 nM E1, 3 μM Ubc9, 24 μM Sumo1 and 2.8 μM SF-1 DBD.

Figure 2

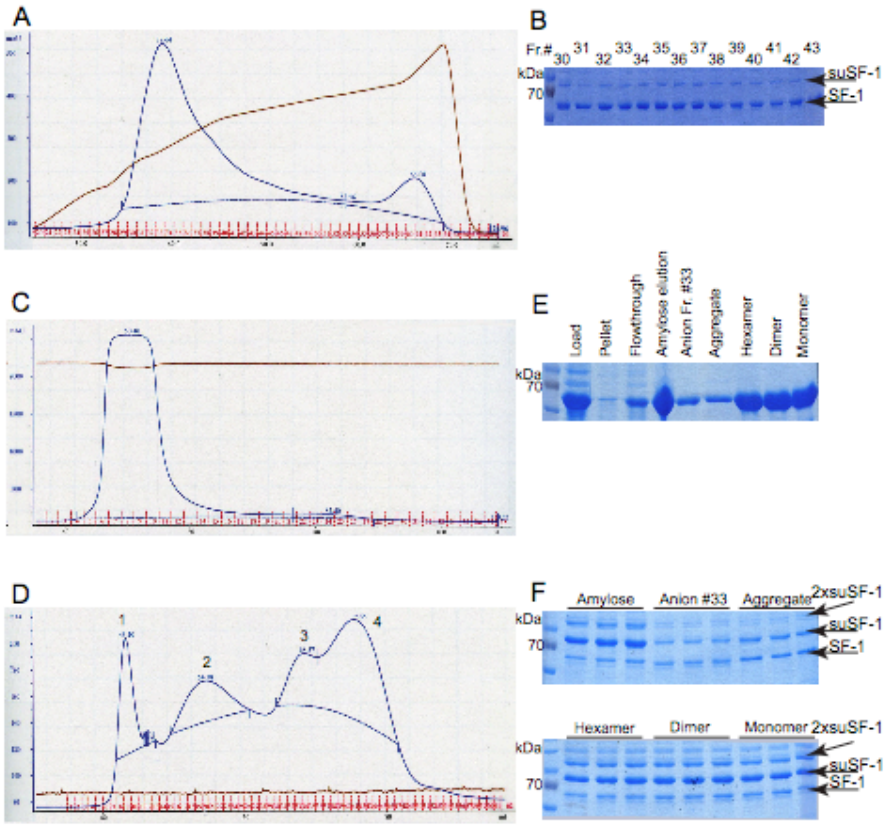
A
B
Fr# 30 31 32 33 34 35 36 37 38 39 40 41 42 43
kDa
70
suSF-1
SF-1
C
E
Load
Pellet
Flowthrough
Amylose elution
Anion Fr. #33
Aggregate
Hexamer
Dimer
Monomer
kDa
70
D
1
2
3
4
F
Amylose
Anion #33
Aggregate
2xsuSF-1
suSF-1
SF-1
kDa
70
Hexamer
Dimer
Monomer
2xsuSF-1
suSF-1
SF-1
kDa
70

Figure 3: In vitro sumoylation optimization. (A) Coommassie stained, IVS timecourse with 140 nM E1, 3 μM Ubc9, and 24 μM SUMO1 or SUMO2. (B) Coommassie stained, IVS timecourse with increasing amounts of SUM02, 140 nM E1 and 5 μM Ubc9. (C) Coommassie stained, IVS timecourse comparing 15' pre-loaded 140 nM E1, 5 μM Ubc9, 20 μM SUMO1 then 1 μM DBD versus all added at the same time. (D) Coommassie stained, IVS timecourse comparing 15' pre-loaded 140 nM E1, 5 μM Ubc9, 20 μM SUMO2 then 1 μM DBD versus all added at the same time. (E) Coommassie stained, IVS timecourse comparing 15' pre-loaded 140 nM E1, 5 μM Ubc9, 20 μM SUMO1 then 1 μM LBD versus added all at the same time. (F) (Top) FTZ-F1 sequence of SF-1 DBD, with SUMOplot predicted substrate lysines underlined in red. (Bottom) Coommassie stained IVS of WT DBD versus K119A and K106R mutants. (G) ^{32}P labeled-SUMO1 autoradiograph comparing the Tris-HCL-based IVS buffer versus the HEPES-based buffer (20 μL reaction)

Figure 3

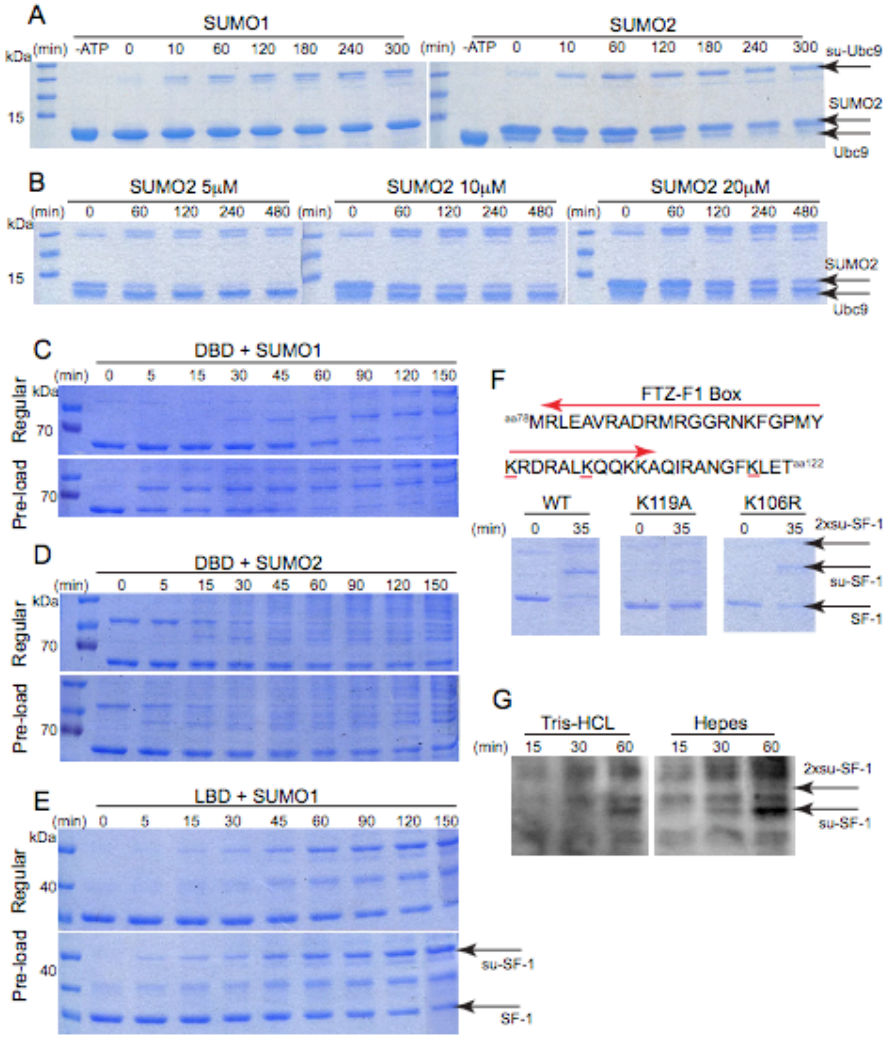
A
SUMO1
SUMO2
(min) -ATP 0 10 60 120 180 240 300
kDa
15
su-Ubc9
SUMO2
Ubc9
B
SUMO2 5μM
SUMO2 10μM
SUMO2 20μM
(min) 0 60 120 240 480
kDa
15
SUMO2
Ubc9
C
DBD + SUMO1
(min) 0 5 15 30 45 60 90 120 150
kDa
Regular
Pre-load
70
D
DBD + SUMO2
(min) 0 5 15 30 45 60 90 120 150
kDa
Regular
Pre-load
70
E
LBD + SUMO1
(min) 0 5 15 30 45 60 90 120 150
kDa
Regular
Pre-load
40
su-SF-1
SF-1
F
FTZ-F1 Box
aa78MRLEAVRADRMRGGRNKFGPMY
KRDRALKQQKKAQIRANGFKLETaa122
WT
K119A
K106R
(min) 0 35
2xsu-SF-1
su-SF-1
SF-1
G
Tris-HCL
Hepes
(min) 15 30 60
2xsu-SF-1
su-SF-1

Figure 4: Sumoylation affects SF-1 DNA binding. (A) Panel of tested SF-1 response elements. While only the core SF-1 bindings sequence is shown, each ds oligo is actually 51 bp long, SHH bs#1 is a 33 mer sequence, hence the slightly faster migration. (B) EMSA of sumoylated or Ulp1 treated SF-1 then bound to 10 μM of putative SF-1 response elements. The bottom panel is the corresponding Coommassie stained gel. Second panel is a control EMSA indicating the specificity of SF-1 as the only DNA-binding protein in the IVS reaction. (C) (Top) EMSA and Coommassie stained gels of WT SF-1 testing the six potential SHH response elements. (Bottom) K119A binding of the same sequences to determine what the slowest migrating band in the WT EMSA corresponds to (cryptic sumoylation of the DBD construct).

Figure 4

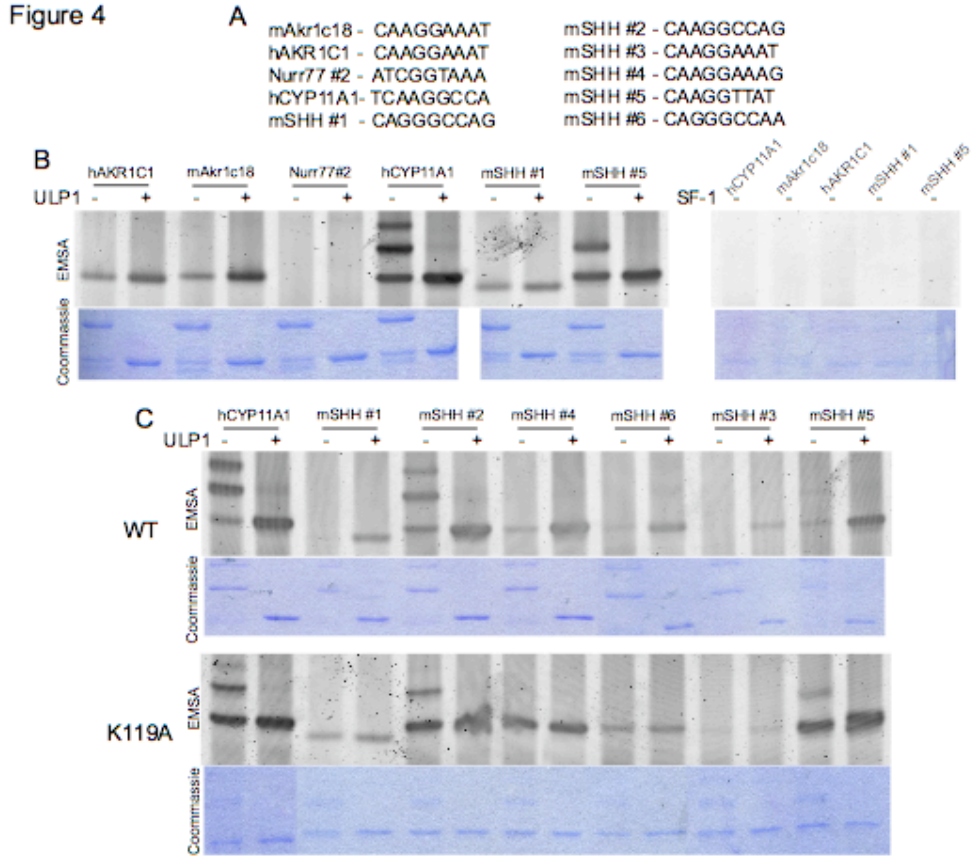
A
mAkr1c18 - CAAGGAAAT
hAKR1C1 - CAAGGAAAT
Nurr77 #2 - ATCGGTAAA
hCYP11A1- TCAAGGCCA
mSHH #1 - CAGGGCCAG
mSHH #2 - CAAGGCCAG
mSHH #3 - CAAGGAAAT
mSHH #4 - CAAGGAAAG
mSHH #5 - CAAGGTTAT
mSHH #6 - CAGGGCCAA
B
hAKR1C1
mAkr1c18
Nurr77#2
hCYP11A1
mSHH #1
mSHH #5
ULP1
SF-1
EMSA
Coommassie
C
hCYP11A1
mSHH #1
mSHH #2
mSHH #4
mSHH #6
mSHH #3
mSHH #5
ULP1
WT
K119A
EMSA
Coommassie

Figure 5: The R114Q human mutation does not affect sumoylation of the SF-1 DBD. (A) IVS timecourse, Coommassie stained gel of WT DBD versus R114Q mutant using SUMO1. (B) IVS timecourse, Coommassie stained gel of WT DBD versus R114Q mutant using SUMO2. (C) DBD and R114Q are first bound to ds MIS oligo, then subjected to a 1.5 hour SUMO1 IVS reaction, visualized via Coommassie staining. (D) (Top) EMSA of sumoylated or Ulp1-treated R114Q mutant bound to SHH response elements. (Bottom) Corresponding SDS PAGE, Coommassie stained.

Figure 5

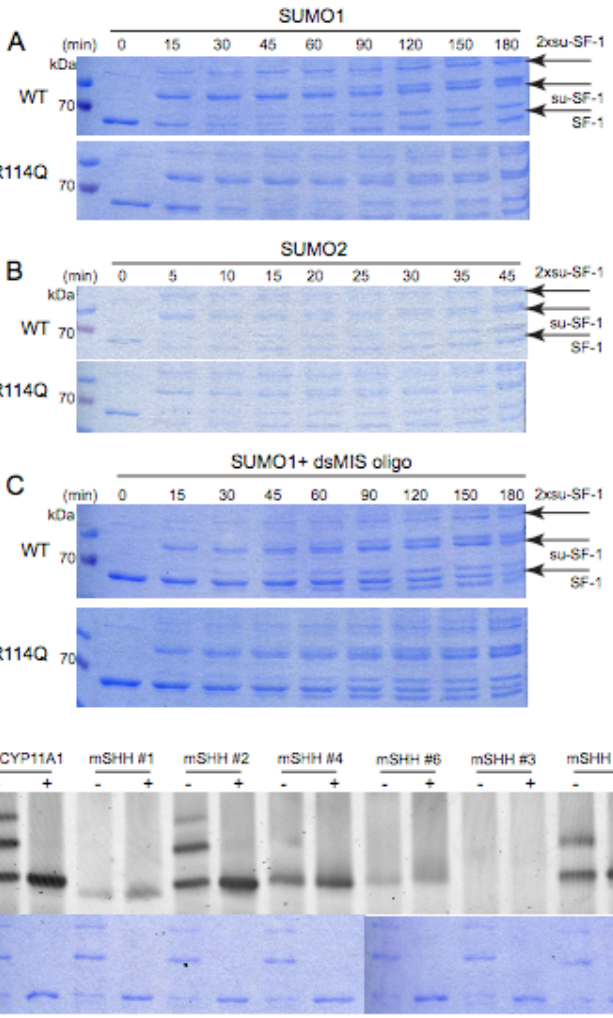
A
SUMO1
(min) 0 15 30 45 60 90 120 150 180
2xsu-SF-1
kDa
WT
70
su-SF-1
SF-1
R114Q
70
B
SUMO2
(min) 0 5 10 15 20 25 30 35 45
2xsu-SF-1
kDa
WT
70
su-SF-1
SF-1
R114Q
70
C
SUMO1+ dsMIS oligo
(min) 0 15 30 45 60 90 120 150 180
2xsu-SF-1
kDa
WT
70
su-SF-1
SF-1
R114Q
70

D
hCYP11A1
mSHH #1
mSHH #2
mSHH #4
mSHH #6
mSHH #3
mSHH #5
ULP1
- + - + - + - + - + - + - +
EMSA
Coommassie

Figure 6: Development of radioactive in vitro sumoylation assays. (A) Autoradiograph of ^{35}S-Methionine labeled SUMO1. First lane, IVTT SUMO1, then incubation with 30 units of Ulp1 protease, flowthrough after 30' incubation with Nickel beads, washes with SUMO1 purification buffer, 1 μL of TEV cleaved SUMO1, 9 μL of the same eluent, 300 mM imidazole elutions from the Nickel beads 1 and 2. (B) Time course autoradiograph of ^{35}S-labeled SUMO1 and SUMO2 used in 20 μL IVS reactions. (C) Generation of ^{32}P labeled SUMO1 and SUMO2. First lane, labeling of the GST-tagged sumo moiety with ^{32}P by PKA, then eluate post G-35 nucleic acid column, TEV cleaved sumo moiety post heat purification. (D) Coommassie stained gel of non-radioactive sumo moieties purified alongside ^{32}P-labeled proteins.

Figure 6

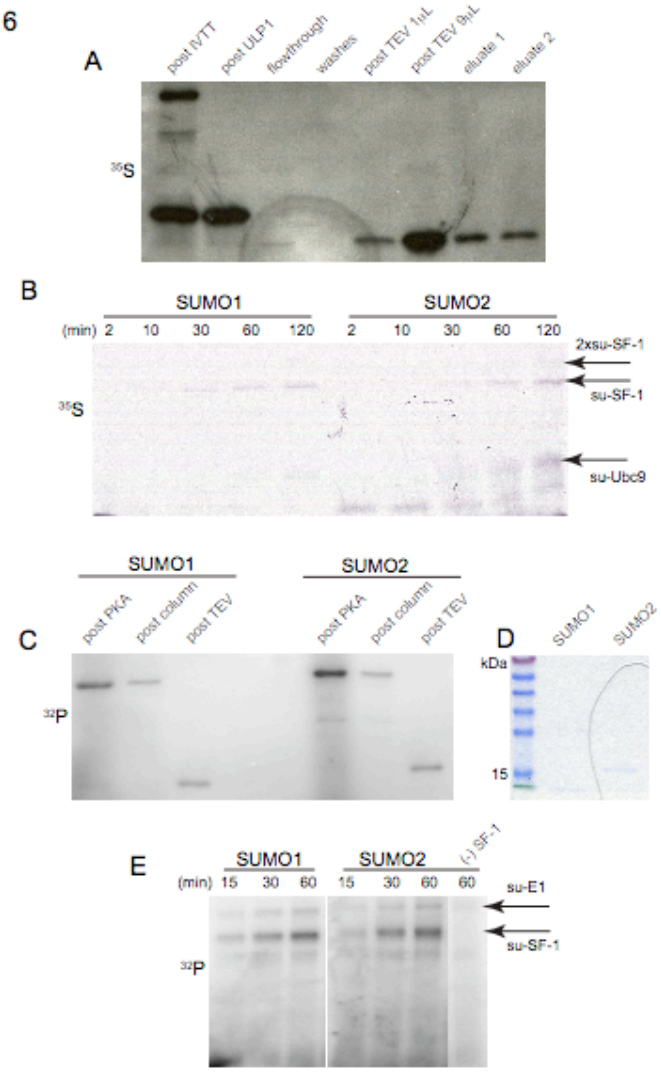
A
post IVTT
post ULP1
flowthrough
washes
post TEV 1µL
post TEV 9µL
eluate 1
eluate 2
35S
B
SUMO1
SUMO2
(min) 2 10 30 60 120 2 10 30 60 120
2xsu-SF-1
su-SF-1
35S
su-Ubc9
C
SUMO1
SUMO2
post PKA
post column
post TEV
post PKA
post column
post TEV
32P
D
SUMO1
SUMO2
kDa
15
E
SUMO1
SUMO2
(-) SF-1
(min) 15 30 60 15 30 60 60
su-E1
su-SF-1
32P

Figure 7: Sumoylation of LRH-1 Hinge-LBD. (A) Space-filled model of LRH-1 Hinge-LBD (cyan)/ β-catenin (green) complex. The final model is refined to 2.8 angstrom with R_{free}/R values of 24.7/20.1. Protein fragments spanned aa138-663 for β-catenin and aa191-541 for LRH-1. (B) Time course IVS reaction of substrates 1) LRH-1 alone, 2) LRH-1/β-catenin pre-formed complex and 3) LRH-1/β-catenin gel-filtration formed complex. Visualized via Coommassie staining (60 μL reactions).

Figure 7

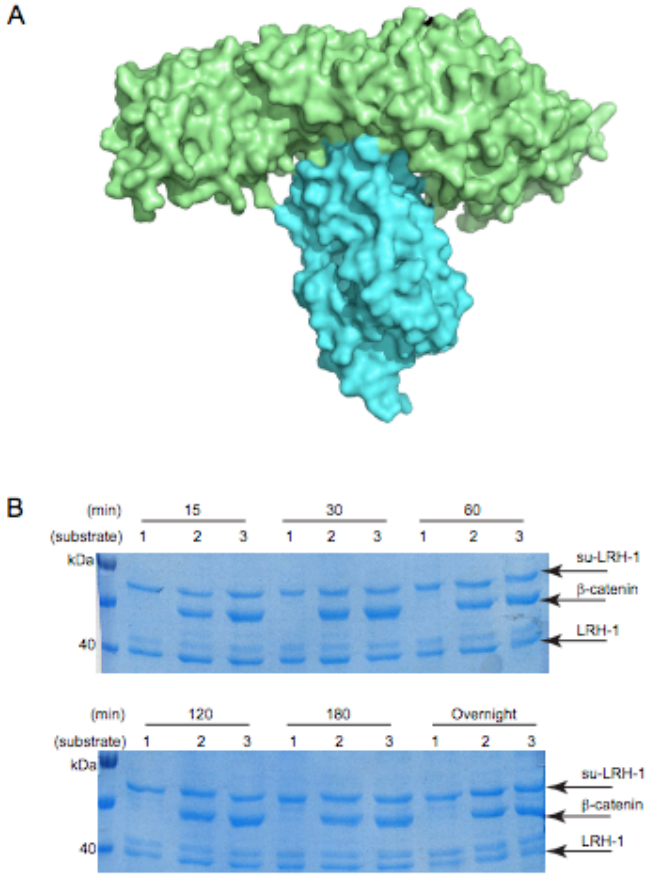
A
B
(min)
15
30
60
(substrate)
1 2 3 1 2 3 1 2 3
kDa
su-LRH-1
β-catenin
LRH-1
40
(min)
120
180
Overnight
(substrate)
1 2 3 1 2 3 1 2 3
kDa
su-LRH-1
β-catenin
LRH-1
40

Figure 8: Purification and sumoylation of full-length SF-1. (A) Gel filtration trace of full-length SF-1 (blue line) with corresponding peaks 1) aggregates, 2) hCYP7A oligo stabilized SF-1 3) degradation products 4) free, excess ds hCYP7A oligo. (B) hCYP7A oligo sequence utilized to stabilize full-length SF-1. (C) Timecourse IVS, comparing SUMO1 versus SUMO2 rates on full-length SF-1. Visualized via Coommassie staining. (D) After overnight incubation of full-length SF-1 with 10-fold excess of ds 51bp MIS of CYP11A1 oligo in an effort to switch out the stabilizing DNA sequence, SUMO1 and SUMO2 rates of modification where then compared. Visualized via Coommassie staining.

Figure 8

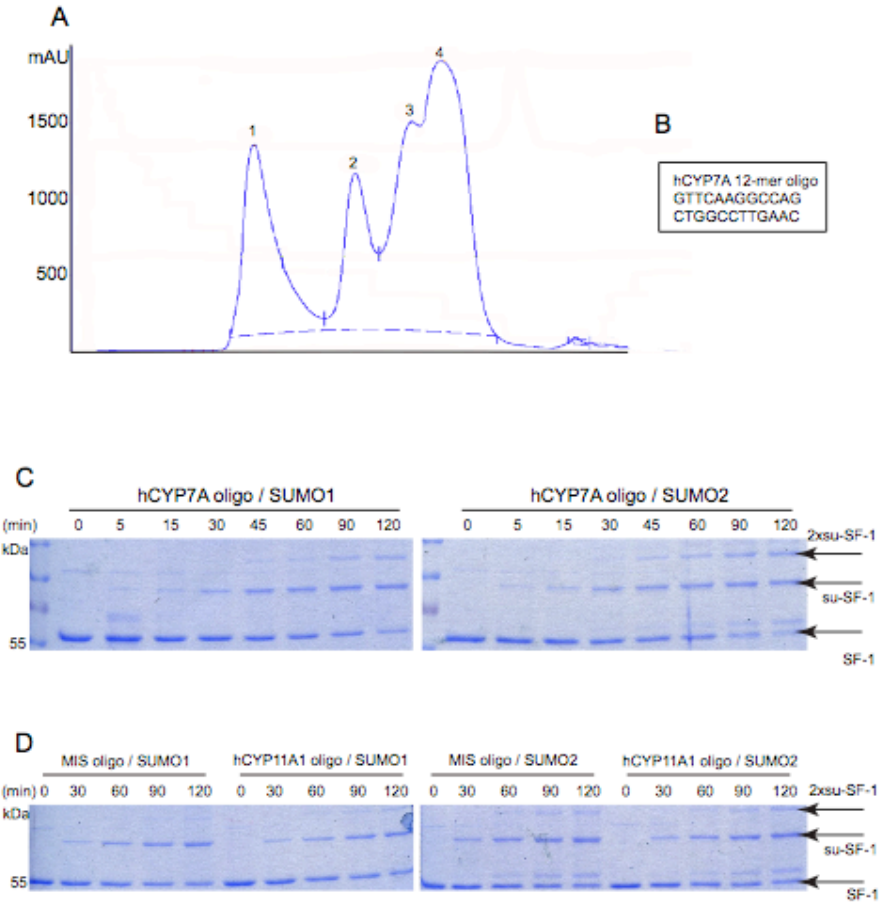
A
mAU
1500
1000
500
1
2
3
4
B
hCYP7A 12-mer oligo
GTTCAAGGCCAG
CTGGCCTTGAAC
C
hCYP7A oligo / SUMO1
hCYP7A oligo / SUMO2
(min) 0 5 15 30 45 60 90 120
kDa
55
2xsu-SF-1
su-SF-1
SF-1
D
MIS oligo / SUMO1
hCYP11A1 oligo / SUMO1
MIS oligo / SUMO2
hCYP11A1 oligo / SUMO2
(min) 0 30 60 90 120
kDa
55
2xsu-SF-1
su-SF-1
SF-1

Figure 9: PIASγ fragment purification and effects on SF-1 DBD sumoylation. (A) (Top) Schematic of the PIASγ protein and fragments and (Bottom) the GST-tagged fragments purified from bacteria. (B) IVS reaction of SF-1 DBD with increasing amounts of GST control or PIASγ proteins, coommassie stained. (C) Timecourse of SF-1 DBD IVS reactions (+/-) 10 μM of ds MIS oligos. 3 μM GST or PIASγ fragments were added to each reaction and visualized via Coommassie staining.

Figure 9

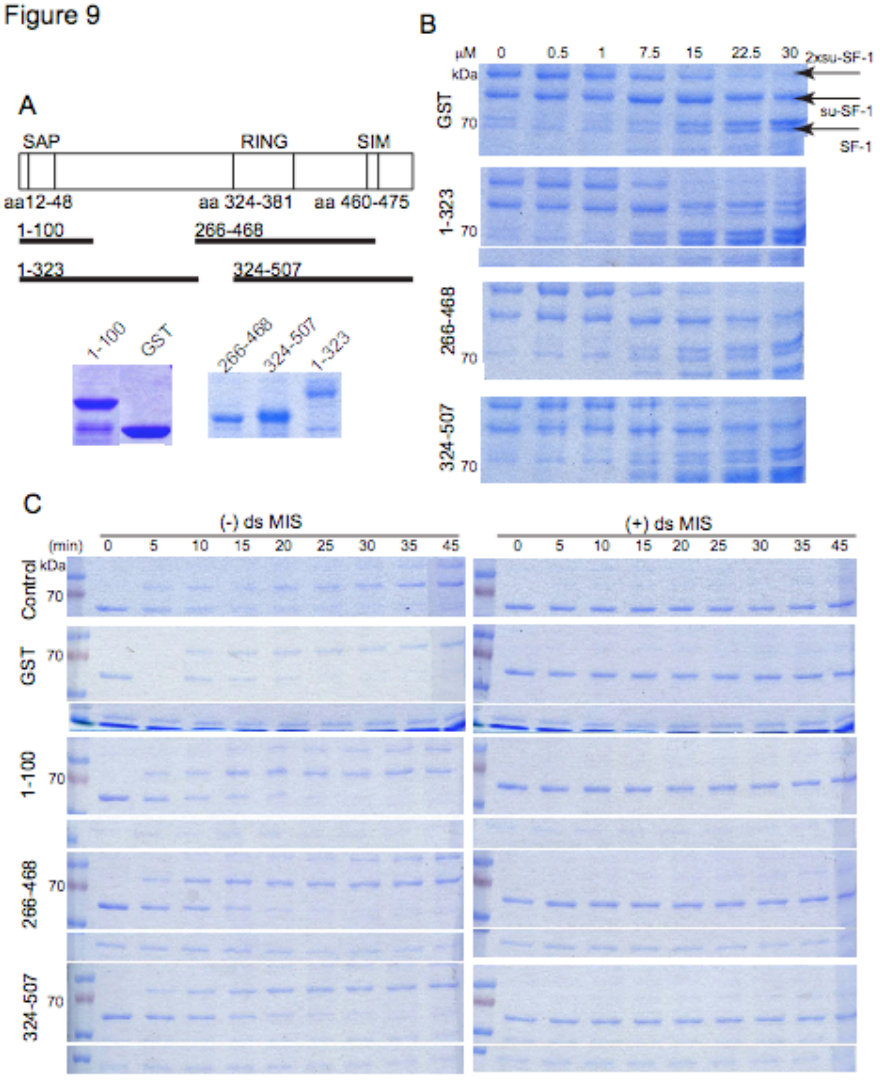
A
SAP
RING
SIM
aa12-48
aa 324-381
aa 460-475
1-100
266-468
1-323
324-507
1-100
GST
266-468
324-507
1-323
B
μM 0 0.5 1 7.5 15 22.5 30
kDa
2xsu-SF-1
su-SF-1
SF-1
GST
1-323
266-468
324-507
70
C
(-) ds MIS
(+) ds MIS
(min) 0 5 10 15 20 25 30 35 45
kDa
Control
GST
1-100
266-468
324-507
70

Figure 10: Full-length PIASγ purification and activity. (A) Tet induction of PIASγ expression in HEK293 cells colocalize with nuclear marker DAPI. (B) Purification of PIASγ involves nuclear extraction and subsequent FLAG- affinity purification. (Top) Western blot α-FLAG of purified PIASγ samples: 1) whole cell lysate, 2) cytosolic fraction, 3) nuclear fraction, 4) hypertonic supernatant, 5) hypertonic pellet, 6) dialysate, 7) flowthrough post M2 beads incubation, 8) washes, 9) eluate #1, 10) eluate #2, 11) eluate #3, 12) M2 beads. (Bottom) Coommassie stained gel of eluates #1-3. (C) Timecourse of PCNA sumoylation (+/-) PIASγ, visualized by Coommassie staining.

Figure 10

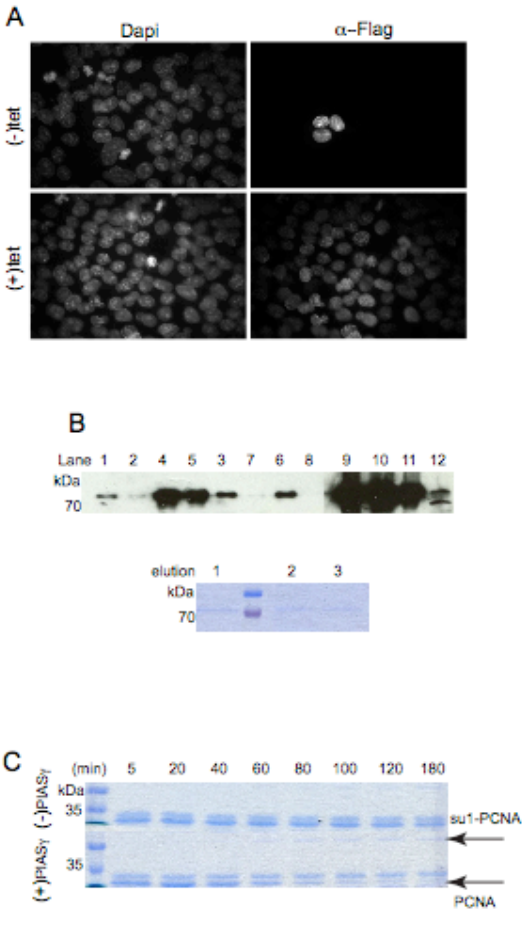
A
Dapi
α-Flag
(-)tet
(+)tet
B
Lane 1 2 4 5 3 7 6 8 9 10 11 12
kDa
70
elution 1 2 3
kDa
70
C
(min) 5 20 40 60 80 100 120 180
kDa
35
35
(-)PIASγ
(+)PIASγ
su1-PCNA
PCNA

Figure 11: PIASγ effects on Sf-1 sumoylation. (A) ^{32}P labeled SUMO1 and SUMO2 autoradiograph of full- length SF-1 with increasing amounts of PIASγ. (B) (Top) ^{32}P labeled SUMO1 autoradiograph of full-length SF-1 IVS (+/-) 100 nM PIASγ. (Bottom) experimental quantitation via IMAGEquant software. (C) ^{32}P labeled SUMO1 and SUMO2 autoradiograph of full- length SF-1 (+/-) stabilizing hCYP7A oligo and (+/-) PIASγ. (D) SF-1 DBD pre-incubated (+/-) ds MIS oligo then IVS (+/-) PIASγ, visualized via Coommassie staining.

Figure 11

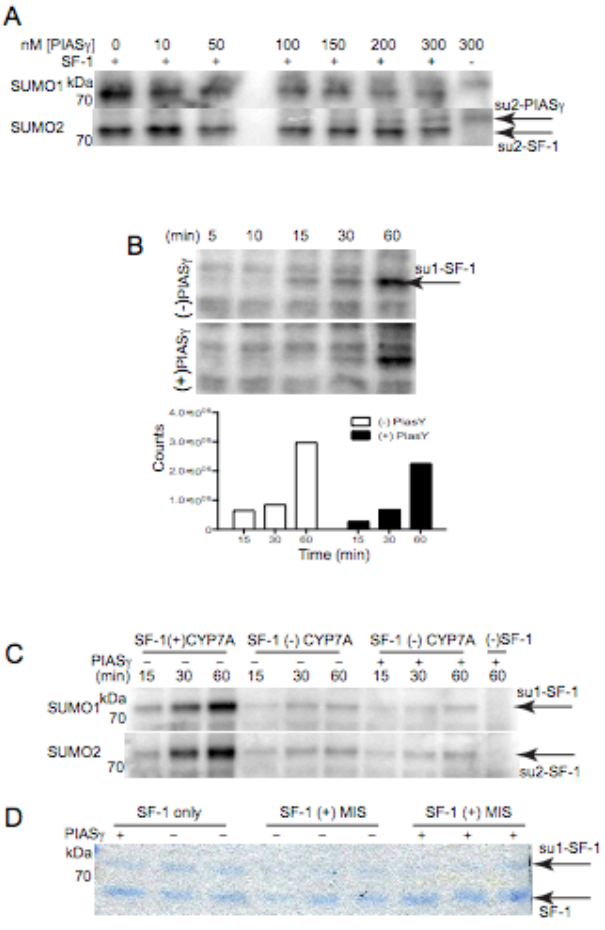
A
nM [PIASγ] 0 10 50 100 150 200 300 300
SF-1 + + + + + + + -
SUMO1 kDa
70
SUMO2
70
su2-PIASγ
su2-SF-1
B
(min) 5 10 15 30 60
(-)PIASγ
(+)PIASγ
su1-SF-1
Counts
(-) PIasY
(+) PIasY
Time (min)
C
SF-1(+)CYP7A SF-1 (-) CYP7A SF-1 (-) CYP7A (-)SF-1
PIASγ
(min) 15 30 60 15 30 60 15 30 60 60
SUMO1 kDa
70
SUMO2
70
su1-SF-1
su2-SF-1
D
SF-1 only SF-1 (+) MIS SF-1 (+) MIS
PIASγ
kDa
70
su1-SF-1
SF-1

References:

1. Sonoda, J., Pei, L. and Evans, R.M. (2008) Nuclear receptors: decoding metabolic disease. *FEBS letters*, **582**, 2-9.
2. Pratt, W.B. and Toft, D.O. (1997) Steroid receptor interactions with heat shock protein and immunophilin chaperones. *Endocrine reviews*, **18**, 306-360.
3. Li, Y., Lambert, M.H. and Xu, H.E. (2003) Activation of nuclear receptors: a perspective from structural genomics. *Structure*, **11**, 741-746.
4. Wilson, T.E., Fahrner, T.J. and Milbrandt, J. (1993) The orphan receptors NGFI-B and steroidogenic factor 1 establish monomer binding as a third paradigm of nuclear receptor-DNA interaction. *Molecular and cellular biology*, **13**, 5794-5804.
5. Parker, K.L., Rice, D.A., Lala, D.S., Ikeda, Y., Luo, X., Wong, M., Bakke, M., Zhao, L., Frigeri, C., Hanley, N.A. *et al*. (2002) Steroidogenic factor 1: an essential mediator of endocrine development. *Recent progress in hormone research*, **57**, 19-36.
6. Luo, X., Ikeda, Y. and Parker, K.L. (1994) A cell-specific nuclear receptor is essential for adrenal and gonadal development and sexual differentiation. *Cell*, **77**, 481-490.
7. Ikeda, Y., Luo, X., Abbud, R., Nilson, J.H. and Parker, K.L. (1995) The nuclear receptor steroidogenic factor 1 is essential for the formation of the ventromedial hypothalamic nucleus. *Molecular endocrinology (Baltimore, Md*, **9**, 478-486.
8. Aigueperse, C., Val, P., Pacot, C., Darne, C., Lalli, E., Sassone-Corsi, P., Veyssiere, G., Jean, C. and Martinez, A. (2001) SF-1 (steroidogenic factor-1), C/EBPbeta (CCAAT/enhancer binding protein), and ubiquitous transcription factors NF1 (nuclear factor 1) and Sp1 (selective promoter factor 1) are required for regulation of the mouse aldose reductase-like gene (AKR1B7) expression in adrenocortical cells. *Molecular endocrinology (Baltimore, Md*, **15**, 93-111.
9. Zimmermann, S., Schwarzler, A., Buth, S., Engel, W. and Adham, I.M. (1998) Transcription of the Leydig insulin-like gene is mediated by steroidogenic factor-1. *Molecular endocrinology (Baltimore, Md*, **12**, 706-713.
10. Little, T.H., Zhang, Y., Matulis, C.K., Weck, J., Zhang, Z., Ramachandran, A., Mayo, K.E. and Radhakrishnan, I. (2006) Sequence-specific deoxyribonucleic acid (DNA) recognition by steroidogenic factor 1: a helix at the carboxy terminus of the DNA binding domain is necessary for complex stability. *Molecular endocrinology (Baltimore, Md*, **20**, 831-843.
11. Solomon, I.H., Hager, J.M., Safi, R., McDonnell, D.P., Redinbo, M.R. and Ortlund, E.A. (2005) Crystal structure of the human LRH-1 DBD-DNA complex reveals Ftz-F1 domain positioning is required for receptor activity. *Journal of molecular biology*, **354**, 1091-1102.
12. Krylova, I.N., Sablin, E.P., Moore, J., Xu, R.X., Waitt, G.M., MacKay, J.A., Juzumiene, D., Bynum, J.M., Madauss, K., Montana, V. *et al*. (2005) Structural analyses reveal phosphatidyl inositols as ligands for the NR5 orphan receptors SF-1 and LRH-1. *Cell*, **120**, 343-355.
13. Hammer, G.D., Krylova, I., Zhang, Y., Darimont, B.D., Simpson, K., Weigel, N.L. and Ingraham, H.A. (1999) Phosphorylation of the nuclear receptor SF-1

modulates cofactor recruitment: integration of hormone signaling in reproduction and stress. *Molecular cell*, **3**, 521-526.
14. Lee, M.B., Lebedeva, L.A., Suzawa, M., Wadekar, S.A., Desclozeaux, M. and Ingraham, H.A. (2005) The DEAD-box protein DP103 (Ddx20 or Gemin-3) represses orphan nuclear receptor activity via SUMO modification. *Molecular and cellular biology*, **25**, 1879-1890.
15. Campbell, L.A., Faivre, E.J., Show, M.D., Ingraham, J.G., Flinders, J., Gross, J.D. and Ingraham, H.A. (2008) Decreased recognition of SUMO-sensitive target genes following modification of SF-1 (NR5A1). *Molecular and cellular biology*, **28**, 7476-7486.
16. Matunis, M.J., Wu, J. and Blobel, G. (1998) SUMO-1 modification and its role in targeting the Ran GTPase-activating protein, RanGAP1, to the nuclear pore complex. *The Journal of cell biology*, **140**, 499-509.
17. Saitoh, H. and Hinchey, J. (2000) Functional heterogeneity of small ubiquitin-related protein modifiers SUMO-1 versus SUMO-2/3. *The Journal of biological chemistry*, **275**, 6252-6258.
18. Li, S.J. and Hochstrasser, M. (1999) A new protease required for cell-cycle progression in yeast. *Nature*, **398**, 246-251.
19. Rodriguez, M.S., Dargemont, C. and Hay, R.T. (2001) SUMO-1 conjugation in vivo requires both a consensus modification motif and nuclear targeting. *The Journal of biological chemistry*, **276**, 12654-12659.
20. Tanaka, H., Tanaka, K., Murakami, H. and Okayama, H. (1999) Fission yeast cdc24 is a replication factor C- and proliferating cell nuclear antigen-interacting factor essential for S-phase completion. *Molecular and cellular biology*, **19**, 1038-1048.
21. Huang, T.T., Wuerzberger-Davis, S.M., Wu, Z.H. and Miyamoto, S. (2003) Sequential modification of NEMO/IKKgamma by SUMO-1 and ubiquitin mediates NF-kappaB activation by genotoxic stress. *Cell*, **115**, 565-576.
22. Johnson, E.S. (2004) Protein modification by SUMO. *Annual review of biochemistry*, **73**, 355-382.
23. Hay, R.T. (2005) SUMO: a history of modification. *Molecular cell*, **18**, 1-12.
24. Knipscheer, P., Flotho, A., Klug, H., Olsen, J.V., van Dijk, W.J., Fish, A., Johnson, E.S., Mann, M., Sixma, T.K. and Pichler, A. (2008) Ubc9 sumoylation regulates SUMO target discrimination. *Molecular cell*, **31**, 371-382.
25. Capili, A.D. and Lima, C.D. (2007) Taking it step by step: mechanistic insights from structural studies of ubiquitin/ubiquitin-like protein modification pathways. *Current opinion in structural biology*, **17**, 726-735.
26. Pichler, A., Gast, A., Seeler, J.S., Dejean, A. and Melchior, F. (2002) The nucleoporin RanBP2 has SUMO1 E3 ligase activity. *Cell*, **108**, 109-120.
27. Kagey, M.H., Melhuish, T.A. and Wotton, D. (2003) The polycomb protein Pc2 is a SUMO E3. *Cell*, **113**, 127-137.
28. Liu, B., Liao, J., Rao, X., Kushner, S.A., Chung, C.D., Chang, D.D. and Shuai, K. (1998) Inhibition of Stat1-mediated gene activation by PIAS1. *Proceedings of the National Academy of Sciences of the United States of America*, **95**, 10626-10631.
29. Liao, J., Fu, Y. and Shuai, K. (2000) Distinct roles of the NH2- and COOH-terminal domains of the protein inhibitor of activated signal transducer and

activator of transcription (STAT) 1 (PIAS1) in cytokine-induced PIAS1-Stat1 interaction. *Proceedings of the National Academy of Sciences of the United States of America*, **97**, 5267-5272.
30. Jimenez-Lara, A.M., Heine, M.J. and Gronemeyer, H. (2002) PIAS3 (protein inhibitor of activated STAT-3) modulates the transcriptional activation mediated by the nuclear receptor coactivator TIF2. *FEBS letters*, **526**, 142-146.
31. Tan, J.A., Hall, S.H., Hamil, K.G., Grossman, G., Petrusz, P. and French, F.S. (2002) Protein inhibitors of activated STAT resemble scaffold attachment factors and function as interacting nuclear receptor coregulators. *The Journal of biological chemistry*, **277**, 16993-17001.
32. Sachdev, S., Bruhn, L., Sieber, H., Pichler, A., Melchior, F. and Grosschedl, R. (2001) PIASy, a nuclear matrix-associated SUMO E3 ligase, represses LEF1 activity by sequestration into nuclear bodies. *Genes & development*, **15**, 3088-3103.
33. Schmidt, D. and Muller, S. (2002) Members of the PIAS family act as SUMO ligases for c-Jun and p53 and repress p53 activity. *Proceedings of the National Academy of Sciences of the United States of America*, **99**, 2872-2877.
34. Kotaja, N., Karvonen, U., Janne, O.A. and Palvimo, J.J. (2002) PIAS proteins modulate transcription factors by functioning as SUMO-1 ligases. *Molecular and cellular biology*, **22**, 5222-5234.
35. Yunus, A.A. and Lima, C.D. (2009) Structure of the Siz/PIAS SUMO E3 ligase Siz1 and determinants required for SUMO modification of PCNA. *Molecular cell*, **35**, 669-682.
36. Schimmer, B.P. and White, P.C. Minireview: steroidogenic factor 1: its roles in differentiation, development, and disease. *Molecular endocrinology (Baltimore, Md*, **24**, 1322-1337.
37. Reverter, D. and Lima, C.D. (2005) Insights into E3 ligase activity revealed by a SUMO-RanGAP1-Ubc9-Nup358 complex. *Nature*, **435**, 687-692.
38. Botrugno, O.A., Fayard, E., Annicotte, J.S., Haby, C., Brennan, T., Wendling, O., Tanaka, T., Kodama, T., Thomas, W., Auwerx, J. *et al*. (2004) Synergy between LRH-1 and beta-catenin induces G1 cyclin-mediated cell proliferation. *Molecular cell*, **15**, 499-509.
39. Yang, F.M., Pan, C.T., Tsai, H.M., Chiu, T.W., Wu, M.L. and Hu, M.C. (2009) Liver receptor homolog-1 localization in the nuclear body is regulated by sumoylation and cAMP signaling in rat granulosa cells. *The FEBS journal*, **276**, 425-436.
40. Fordyce, P.M., Gerber, D., Tran, D., Zheng, J., Li, H., DeRisi, J.L. and Quake, S.R. De novo identification and biophysical characterization of transcription-factor binding sites with microfluidic affinity analysis. *Nature biotechnology*, **28**, 970-975.
41. Deng, Z., Wan, M. and Sui, G. (2007) PIASy-mediated sumoylation of Yin Yang 1 depends on their interaction but not the RING finger. *Molecular and cellular biology*, **27**, 3780-3792.
42. Kajimura, S., Seale, P., Tomaru, T., Erdjument-Bromage, H., Cooper, M.P., Ruas, J.L., Chin, S., Tempst, P., Lazar, M.A. and Spiegelman, B.M. (2008) Regulation

of the brown and white fat gene programs through a PRDM16/CtBP transcriptional complex. *Genes & development*, **22**, 1397-1409.
43. Ogawa, H., Komatsu, T., Hiraoka, Y. and Morohashi, K. (2009) Transcriptional Suppression by Transient Recruitment of ARIP4 to Sumoylated nuclear receptor Ad4BP/SF-1. *Molecular biology of the cell*, **20**, 4235-4245.
44. Yunus, A.A. and Lima, C.D. (2005) Purification and activity assays for Ubc9, the ubiquitin-conjugating enzyme for the small ubiquitin-like modifier SUMO. *Methods in enzymology*, **398**, 74-87.
45. Zhu, J., Zhu, S., Guzzo, C.M., Ellis, N.A., Sung, K.S., Choi, C.Y. and Matunis, M.J. (2008) Small ubiquitin-related modifier (SUMO) binding determines substrate recognition and paralog-selective SUMO modification. *The Journal of biological chemistry*, **283**, 29405-29415.
46. Song, J., Durrin, L.K., Wilkinson, T.A., Krontiris, T.G. and Chen, Y. (2004) Identification of a SUMO-binding motif that recognizes SUMO-modified proteins. *Proceedings of the National Academy of Sciences of the United States of America*, **101**, 14373-14378.
47. Song, J., Zhang, Z., Hu, W. and Chen, Y. (2005) Small ubiquitin-like modifier (SUMO) recognition of a SUMO binding motif: a reversal of the bound orientation. *The Journal of biological chemistry*, **280**, 40122-40129.
48. Kim, E.T., Kim, K.K., Matunis, M.J. and Ahn, J.H. (2009) Enhanced SUMOylation of proteins containing a SUMO-interacting motif by SUMO-Ubc9 fusion. *Biochemical and biophysical research communications*, **388**, 41-45.
49. Hecker, C.M., Rabiller, M., Haglund, K., Bayer, P. and Dikic, I. (2006) Specification of SUMO1- and SUMO2-interacting motifs. *The Journal of biological chemistry*, **281**, 16117-16127.
50. Gearhart, M.D., Holmbeck, S.M., Evans, R.M., Dyson, H.J. and Wright, P.E. (2003) Monomeric complex of human orphan estrogen related receptor-2 with DNA: a pseudo-dimer interface mediates extended half-site recognition. *Journal of molecular biology*, **327**, 819-832.
51. Palvimo, J.J. (2007) PIAS proteins as regulators of small ubiquitin-related modifier (SUMO) modifications and transcription. *Biochemical Society transactions*, **35**, 1405-1408.
52. Nishida, T. and Yasuda, H. (2002) PIAS1 and PIASxalpha function as SUMO-E3 ligases toward androgen receptor and repress androgen receptor-dependent transcription. *The Journal of biological chemistry*, **277**, 41311-41317.
53. Komatsu, T., Mizusaki, H., Mukai, T., Ogawa, H., Baba, D., Shirakawa, M., Hatakeyama, S., Nakayama, K.I., Yamamoto, H., Kikuchi, A. *et al*. (2004) Small ubiquitin-like modifier 1 (SUMO-1) modification of the synergy control motif of Ad4 binding protein/steroidogenic factor 1 (Ad4BP/SF-1) regulates synergistic transcription between Ad4BP/SF-1 and Sox9. *Molecular endocrinology (Baltimore, Md*, **18**, 2451-2462.
54. Rogers, R.S., Horvath, C.M. and Matunis, M.J. (2003) SUMO modification of STAT1 and its role in PIAS-mediated inhibition of gene activation. *The Journal of biological chemistry*, **278**, 30091-30097.
55. Sharrocks, A.D. (2006) PIAS proteins and transcriptional regulation--more than just SUMO E3 ligases? *Genes & development*, **20**, 754-758.

56. Borden, K.L. (2000) RING domains: master builders of molecular scaffolds? *Journal of molecular biology*, **295**, 1103-1112.
57. Ouyang, J., Shi, Y., Valin, A., Xuan, Y. and Gill, G. (2009) Direct binding of CoREST1 to SUMO-2/3 contributes to gene-specific repression by the LSD1/CoREST1/HDAC complex. *Molecular cell*, **34**, 145-154.

Publishing Agreement

It is the policy of the University to encourage the distribution of all theses, dissertations, and manuscripts. Copies of all UCSF theses, dissertations, and manuscripts will be routed to the library via the Graduate Division. The library will make all theses, dissertations, and manuscripts accessible to the public and will preserve these to the best of their abilities, in perpetuity.

Please sign the following statement:

I hereby grant permission to the Graduate Division of the University of California, San Francisco to release copies of my thesis, dissertation, or manuscript to the Campus Library to provide access and preservation, in whole or in part, in perpetuity.

Author Signature

1/5/11

Date